Earth Systems and Environment
https://doi.org/10.1007/s41748-024-00555-1

ORIGINAL ARTICLE

Evaluating Daytime and Nighttime Land Surface Temperature Pattern and Trends in India: A Comparative Analysis of Satellite and Reanalysis Data

Seema Rani[1] · **Subhash Singh**[1] · **Sanju Purohit**[2]

Received: 11 July 2024 / Revised: 8 December 2024 / Accepted: 14 December 2024

Abstract
Land surface temperature (LST) is a highly dynamic and key variable of the Earth's energy budget, which makes it crucial to understand its behavior from global to regional scales. It can be examined across extensive geographic regions using satellite or reanalysis datasets, offering high spatial and temporal resolutions with global coverage. Thus, the present study aims to analyze the comparative spatial distribution and trends in the daytime and nighttime mean LST over the six climatic regions of India for the period 2003–2022 using satellite (MODIS and AIRS Aqua) and reanalysis (ERA5-Land and MERRA-2) datasets. The mean LST of satellites and reanalysis datasets are juxtaposed using various statistical methods, including the correlation coefficient (r), root mean square error (RMSE), percentage bias (Pbias), and mean absolute error (MAE). Additionally, the seasonal and annual LST trends are computed using Theil Sen's Slope Estimator and Contextual Mann-Kendall (CMK) significance test. The findings show a very high correlation (> 0.85) in the daytime and nighttime LST of all four datasets. Furthermore, the RMSE values vary from 2.71 °C to 13.51 °C at an annual scale. However, nighttime LST is more consistent than daytime among the datasets. Across all datasets, a significant cooling trend is observed in annual daytime LST (MODIS Aqua: -0.115 °C/yr to MERRA-2: -0.004 °C/yr), except ERA5-Land (0.004 °C/yr). For annual nighttime LST, all datasets indicate warming, ranging from 0.010 °C/yr (AIRS Aqua) to 0.049 °C/yr (MODIS Aqua), except MERRA-2 (-0.003 °C/yr). Annual daytime mean LST shows a cooling trend across most of the regions, with the largest decline in the North-West (-0.070 °C/yr) and West-Central (-0.064 °C/yr). In contrast, North-East (0.009 °C/yr) and Himalayan Region (0.014 °C/yr) regions exhibit slight warming in the daytime mean LST. However, nighttime mean LST indicates warming in all the climatic regions, except the Himalayan Region (-0.003 °C/yr). Overall, the study suggests the usage of nighttime LST data over daytime LST considering its consistency. The present study aids in refining the comprehension of LST trends, bolstering the credibility of these datasets for climate studies, environmental monitoring, and policy formulation, especially in the diverse landscapes of India.

Keywords AIRS · Contextual Mann-Kendall Significance Test · Daytime/Nighttime Land Surface Temperature · Climatic Regions · ERA5-Land · India · MERRA-2 · MODIS · Theil-Sen Slope Estimator

1 Introduction

Land surface temperature (LST) refers to the quantity of thermal energy usually found within a shallow layer ranging from a few millimeters to a few centimeters beneath the Earth's surface (Liu et al. 2023; Li et al. 2013). It regulates the net radiation budget by enabling the flow of heat and moisture between the terrestrial surface and the atmosphere (Li et al. 2013). It is influenced by both terrestrial and atmospheric factors, and in turn, it impacts the weather and climate system from local to global scales. Its highly

✉ Seema Rani
seemarani@bhu.ac.in

Subhash Singh
subhashsingh@bhu.ac.in

Sanju Purohit
purohitsanjana@icloud.com

[1] Department of Geography, Institute of Science, Banaras Hindu University, Varanasi, Uttar Pradesh, India

[2] Department of Environmental/Ecological Studies and Sustainability, Akamai University, Waimea, HI 96743, USA

Published online: 18 December 2024

dynamic nature renders it one of the essential climatic variables of Earth's energy exchange, water cycle, and associated environmental processes (GCOS 2016). Understanding spatio-temporal variations of LST offers vital insights into the dynamics of surface energy equilibrium, and serves as a pivotal indicator for environmental health, weather patterns (Dimri 2019), climate variability (Mal et al. 2022), urbanization impact (Cai et al. 2018), etc.

LST can be obtained from three sources: ground-based observations, remote sensing, and reanalysis datasets. Ground-based measurements offer high spatial and temporal accuracy, but they suffer from limited spatio-temporal coverage due to the scarcity and irregular distribution of observing stations (Latif et al. 2020). Therefore, conducting a comprehensive study of LST over a vast region and for an extended period is not feasible with station-based data alone. On a global scale, LST measurements from satellites and reanalysis datasets take precedence due to their superior spatial and temporal resolution (Wang et al. 2022; Liu et al. 2020). Satellite datasets encompass LST data derived from sensors like Landsat, Atmospheric Infrared Sounder (AIRS) Aqua, Moderate Resolution Imaging Spectroradiometer (MODIS), and the Advanced Very High-Resolution Radiometer (AVHRR) aboard the National Oceanic and Atmospheric Administration (NOAA) (Tian et al. 2020; Wan 2019). Among these, satellites offering high spatial resolution data (e.g., Landsat-30 m) but sacrifice temporal resolution (Landsat-16 days), while those emphasizing high temporal resolution (e.g., MODIS-daily) compromise spatial resolution (MODIS-1 km). Satellites are unable to provide data during cloudy weather conditions, which results in missing values and influences the findings. Another option for measuring surface temperatures with great temporal and spatial resolution on a worldwide scale is to use reanalysis datasets (Muñoz-Sabater et al. 2021; Bosilovich et al. 2015). These provide values in all weather conditions, making them more popular and useful in climate-related research. Some frequently used reanalysis datasets in LST investigations are the Modern-Era Retrospective analysis for Research and Applications (MERRA), MERRA-2, European Centre for Medium-Range Weather Forecasts (ECMWF) products (e.g., ERA5, ERA5-Land, etc.), Japanese 55-year Reanalysis (JRA-55), etc. (Wang et al. 2022; Wen et al. 2022; Liu et al. 2020).

The spatial distribution and rate of change in LST at regional and global scales have been widely studied in the past, using satellite and reanalysis datasets (Wang et al. 2022; Liu et al. 2020; Prakash and Norouzi 2020; Susskind et al. 2019; Zhou and Wang 2016). Over a global scale, both MODIS (0.26 °C/decade) and ERA5-Land (0.34 °C/decade) analyzed a warming trend from 2001 to 2020 (Wang et al. 2022). The LST trend derived from MODIS Aqua, AIRS Aqua, and ERA5-Land showed approximately 0.02, 0.03, and 0.04 k/year across the globe from 2003 to 2017 (Liu et al. 2020). Susskind et al. (2019) analyzed the global mean surface temperature using five datasets, including AIRS, Goddard Institute for Space Studies Surface Temperature Analysis (GISTEMP), Hadley Centre/Climatic Research Unit (HadCRUT4), Cowtan and Way (C&W), and ECMWF Interim. Across all datasets, a warming trend (AIRS: 0.24, GISTEMP: 0.22, HadCRUT4: 0.17, C&W: 0.19, and ECMWF: 0.20 °C/decade) was observed from 2003 to 2017. Among continents, Asia exhibits a warming trend of 0.16 °C/decade and 0.20 °C/decade according to MODIS and ERA5-Land, respectively (Wang et al. 2022). The trend from the three datasets, namely MODIS Aqua, AIRS Aqua, and ERA5-Land, varies between −0.2 and 0.2 °C/year across Asia (Liu et al. 2020). Prakash and Norouzi (2020) have found a trend between 2 to −2 °C/decade in daytime and nighttime MODIS LST over different parts of India for 15 years (2003–2017). Susskind et al. (2019) show a cooling trend (range: 0 to −0.5 °C/decade) over most of India using AIRS data (2003–2017). Over the Ganga River Basin, a declining trend of −0.017 °C/year has been observed in the annual mean LST, using the MODIS dataset from 2001 to 2019 (Mal et al. 2022). Rani and Mal (2022) found both cooling and warming trends in daytime LST of MODIS in the western Himalayan region of India compared to eastern Himalaya during 2001–2019. Mal et al. (2023) revealed a consistent increase in daytime mean LST (0.020–0.024 °C/yr) across all seasons except winter and post-monsoon, as well as nighttime LST (0.013–0.049 °C/yr) in the Indus River Basin using MODIS data from 2002 to 2022. Additionally, the analysis indicated a significant divergence between daytime and nighttime LST, with nighttime LST (0.025 °C/yr) rising notably faster than daytime LST (0.0016 °C/yr), suggesting the presence of a distinct nighttime warming effect. In regions with limited data availability, particularly at smaller geographic scales, researchers have observed significant uncertainty arising from notable discrepancies in trends among different LST datasets. Using high-resolution spatial data enables the analysis of geographic patterns associated with localized warming, a crucial aspect for conducting assessments of climate-related risks.

To the best of our knowledge, there hasn't been a comparison of LST trends (daytime and nighttime LST) derived from satellite and reanalysis datasets specific to India, despite the existence of some global studies (Wang et al. 2022; Liu et al. 2020; Zhou and Wang 2016). Therefore, this study aims to accomplish three primary objectives in the present study. Firstly, it seeks to analyze the spatio-temporal distribution of daytime and nighttime mean LST across six climatic regions of India using satellites (MODIS and AIRS

Aqua) and reanalysis (ERA5-Land and MERRA-2) datasets of the period 2003–2022. Secondly, the study aims to analyze inter-dataset variability of LST and compare satellite and reanalysis datasets using various statistical indicators. Lastly, it aims to assess the comparative seasonal/annual trends in daytime and nighttime LST. The present study selected the period from 2003 to 2022 due to the availability of high-quality, continuous satellite and reanalysis data that align with the study objectives. This timeframe includes critical climatic events in India, such as multiple El Niño (2009–2010, 2015–2016) and La Niña (2010-11, 2021–2022) events, as well as significant droughts (2009, 2015) and heatwaves, which are crucial for analyzing long-term LST trends (Mishra 2020; Han and Wang 2021; Null 2024). Knowing that each dataset possesses unique characteristics and employs different algorithms for LST product generation, analyzing multiple datasets will provide a more comprehensive understanding of the appropriate data selection for understanding LST patterns in India. The novelty of this paper lies in the lack of recent studies evaluating daytime and nighttime LST datasets at both global and regional scales. The studies using different LST datasets are almost negligible in the context of the whole of India. The study also provides region-specific insights into LST (daytime and nighttime) behavior by focusing on six diverse climatic regions of India. Such granularity is often overlooked in broader, global studies that fail to capture regional subtleties. The present study uses fine temporal (day vs. night) and spatial scales data, offering insights into regional and diurnal LST variations that were previously unexplored at this level of detail. By identifying discrepancies in trends among datasets, the study underscores the importance of dataset selection and potential biases in trend analysis in India. This study offers a comprehensive evaluation of satellite and reanalysis data, elucidating the respective strengths and limitations of each approach. Further, this comparative analysis serves to deepen comprehension regarding the reliability and accuracy of data, which are crucial for conducting rigorous scientific analyses. Consequently, an improved understanding of LST datasets in India is beneficial for managing natural resources, crop monitoring, urban planning, environmental monitoring, and human health.

2 Data and Method

The present study used four datasets of remote sensing (MODIS Aqua and AIRS Aqua) and reanalysis (ERA-5 Land and MERRA-2) to analyze the spatiotemporal variations in LST across India and compare their results (Table 1;

Table 1 Description of the datasets used in the present study

S.No	Datasets	Type of Data	Spatial Resolution	Temporal Resolution	Spatial Coverage	Period	Processing Method	Source
1.	MODIS Aqua (MYD11A1 v.061 L3)	Satellite	1 km	Daily	Global	May 2002 -Present	Split-window	https://lpdaac.usgs.gov/products/myd11a1v061/
2.	AIRS Aqua (AIRS3STM v006)	Satellite	1° × 1°	Daily	Global	September 2002 - Present	Least squares estimation using Singular Value Decomposition regularization on cloud-cleared radiances on AIRS 3 × 3 fields of regard (FoR)	https://disc.gsfc.nasa.gov/datasets/AIRS3STM_006/summary
3.	MERRA-2	Reanalysis	0.625° × 0.5°	Hourly	Global	1980 - Present	Three-Dimensional Variational (3D-VAR) Goddard Earth Observing System Model, Version 5 (GEOS-5)	https://gmao.gsfc.nasa.gov/reanalysis/merra-2/
4.	ERA5-Land	Reanalysis	0.1° × 0.1°	Hourly	Global	1950 - Present	Four-Dimensional Variational (3D-VAR) Carbon Hydrology-Tiled ECMWF Scheme for Surface Exchanges over Land (CHTESSEL) Model	https://cds.climate.copernicus.eu/

Figs. 1 and 2). All the given LST datasets are obtained for the period 2003–2022 due to data availability and managed consistency in comparison of mean and trend analysis. The present study selects LST datasets based on four criteria: (a) the common period of availability, (b) comparatively higher spatial and temporal resolution, (c) spatial coverage over India, and (d) consistency in data availability. Among satellite datasets, Landsat (30 m) and ASTER (90 m) offer a high spatial resolution, but their temporal resolution is limited to 16-day intervals (Li et al. 2023). Additionally, while VIRS and AVHRR provide both high spatial and temporal resolution, their data is available only from 2012 to 2015 onwards, respectively. Other satellite datasets are available, but they cater to specific regions, such as SEVIRI/MSG for Africa, MTSAT for Japan, and ABI/GOES-R for the Americas. In the case of reanalysis datasets, options such as NCEP-R1 (2.5°×2.5°), NCEP-R2 (2.5°×2.5°), MERRA (0.667°×0.5°), MERRA-Land (0.667°×0.5°), ERA-Interim (0.75° x 0.75°), ERA5 (0.25°×0.25°), and JRA-55 (1.25°×1.25°) provide LST products (Li et al. 2023). However, they generally

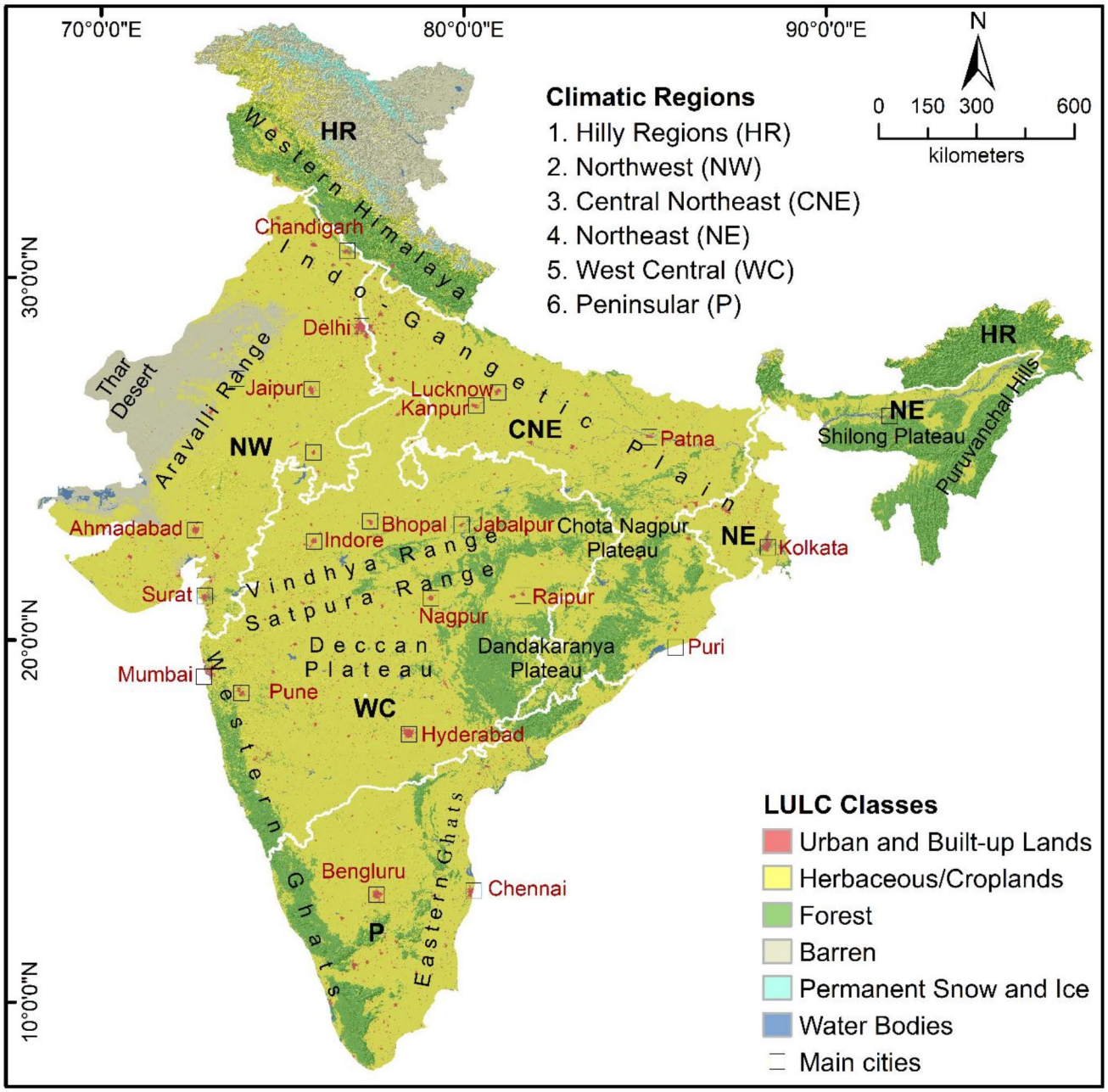

Fig. 1 Extent of India including six climatic regions considered in the present study. The background shows the country's land use/land cover of the year 2022 (derived from MCD12Q1.061 500 m)

have lower spatial resolution as compared to ERA5-Land (0.1°×0.1°) and MERRA-2 (0.625°×0.5°), and some (JRA-55, ERA-Interim, MERRA) are also no longer actively distributing their data. MODIS and AIRS data are affected by cloud cover, while reanalysis data like ERA5-Land and MERRA-2 are based on models, which may introduce bias (retrieval algorithm bias, sensor calibration, number of observations, and modeling assumptions). The present study dataset selection balances these factors to capture both spatial and temporal patterns/trends effectively. It helps the researchers to understand the level of differences based on the data selection, particularly in the heterogeneous climatic and physiographic conditions of India.

2.1 Remote Sensing Data

The study incorporates two satellite datasets (Fig. 2): MODIS Aqua (clear sky) and AIRS Aqua, both having global coverage considering their wider usage in recent times. From MODIS Aqua, the MYD11A1 v.061 level-3 data is chosen which is provided by NASA's Land Processes Distributed Active Archive Center (LP DAAC) from May 2002 onward. Both MODIS and AIRS Aqua have overpass times at 01:30 (nighttime-descending) and 13:30 (daytime-ascending). Wan (2019) mentioned that the C6 MODIS product outperformed the C4.1 and C5. It provides daily per-pixel LST and Emissivity with a pixel size of about 0.01° (1 km). In MOD11A1, the pixel value is derived from the MYD11_L2 swath product. The daytime and nighttime mean LST at seasonal and annual scales are computed by averaging the daily LST_Day_1km and LST_Night_1km values separately. Additionally, Goddard Earth Sciences Data and Information Services Center (GES DISC) monthly AIRS3STM v006 product, AIRS Aqua L3, has been chosen. The standard grided products are available at 1° by 1° from September 2002 and derived from the v6 L2 swath products (Tian et al. 2020). The monthly surface temperature layers (surfskinTemp_A and surfskinTemp_D) have been averaged at seasonal and annual scales. The missing values in the remote sensing data are addressed by averaging daily observations to monthly and then seasonal scales (without interpolation). This approach helps to minimize gaps caused by cloud cover and provides a more comprehensive understanding of the general LST patterns in the study area.

2.2 Reanalysis Data

In addition to satellite data, the study also includes two globally available reanalysis datasets including ERA-5 Land and MERRA-2 (Fig. 2). The Copernicus Climate Change Service (C3S) Climate Data Store (CDS) provides ECMWF ERA5-Land products from 1950 onwards. It is monthly averaged by hour of day and provides skin temperature (SKT) at 0.1° (9 km) horizontal resolution (Muñoz-Sabater et al. 2021). The SKT denotes the theoretical temperature of the Earth's surface necessary to maintain the surface energy balance. It

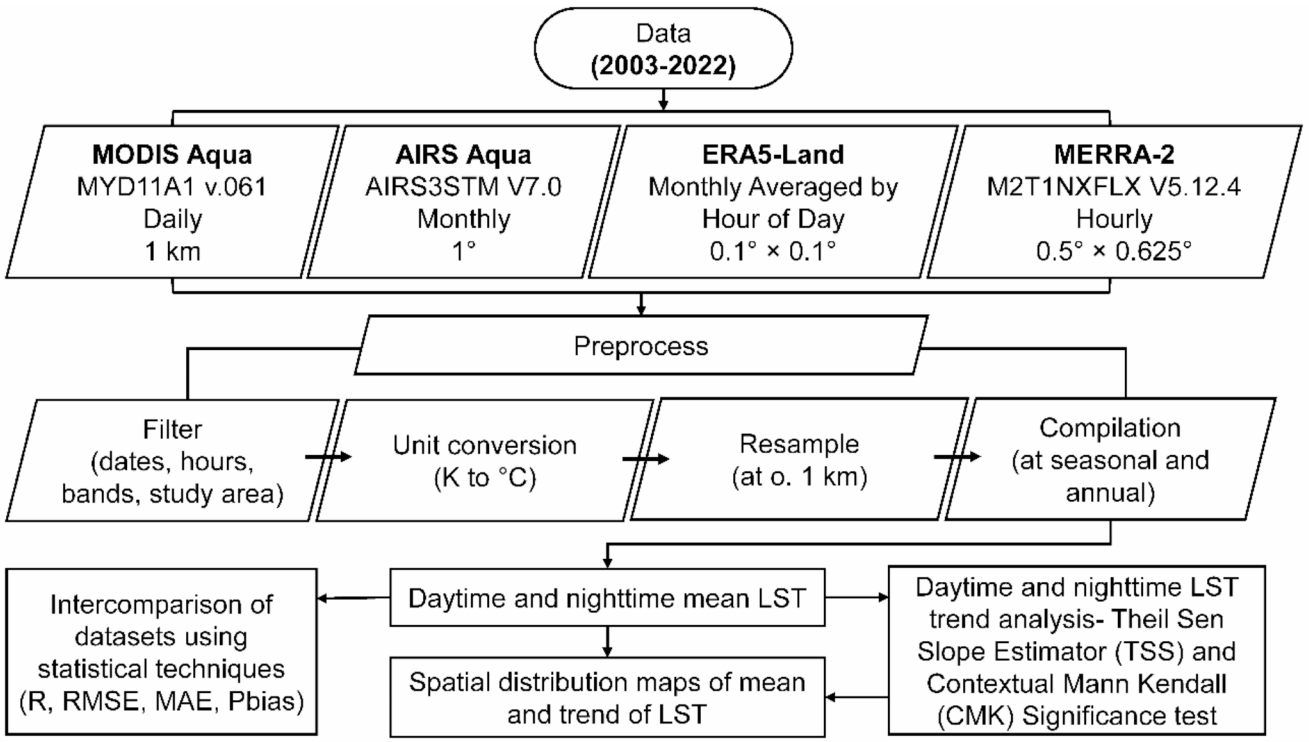

Fig. 2 Methodological framework for the present study

signifies the temperature of the uppermost surface layer (top 7 cm), which lacks heat capacity and can promptly adjust to alterations in surface fluxes (Muñoz-Sabater et al. 2021). To align the ERA5-Land SKT with the satellite LST data, the average of SKT has been taken at 13:00 and 14:00 for daytime and 01:00 and 02:00 for nighttime for each grid cell. Another reanalysis dataset used in the study is the MERRA-2, provided by NASA's Global Modelling and Assimilation Office (GMAO). It employs the Goddard Earth Observing System Model (GEOS) version 5.2.14. The present study has obtained MERRA-2 hourly M2T1NXFLX 'effective surface skin temperature' with longitudinal/latitudinal resolution of 0.625°×0.5° (Bosilovich et al. 2015).

To understand the thermal changes (such as temperature trends) over a large-scale climate system, the maximum and minimum temperatures have been considered more suitable as compared to the mean daily average temperature (Mildrexler et al. 2011). It may be attributed to that, the maximum daily LST exhibits high sensitivity to Earth's energy changes. Thus, the present study selected the MODIS Aqua and AIRS Aqua data, having overpass times of 13:30 (closest to daily maximum: daytime) and 01:30 (closest to daily minimum: nighttime). Furthermore, to align the ERA5-Land with the satellite LST values, the study has taken the average of SKT available at 13:00 and 14:00 for daytime and 01:00 and 02:00 for nighttime for each grid cell. Additionally, for MERRA-2, the related bands (band 2 – 01:30 and band 14 – 13:30) of the product have been extracted.

2.3 Data Processing

The data of MODIS Aqua, AIRS Aqua, ERA5-Land, and MERRA-2 are preprocessed including filtering (date, time, and study area), resampling (to 1 km), and unit conversion (kelvin to °C) (Fig. 2). All the preprocessed data are compiled at seasonal and annual scales, following the Indian Meteorological Department (IMD 2023) seasonal classification i.e., January to February (winter), March to May (pre-monsoon), June to September (monsoon), and October to December (post-monsoon) (IMD 2023). Furthermore, descriptive statistics of seasonal/annual daytime and nighttime mean LST are calculated to understand its spatial and temporal variability across India from 2003 to 2022.

2.4 Comparative Statistical Indicators

After the mean estimation of daytime and nighttime mean LST of India, the intercomparison of all four datasets is done using statistical indicators, including the correlation coefficient (R), root mean square error (RMSE), percentage bias (Pbias), and mean absolute error (MAE) (Fig. 2). The corresponding equations for these parameters are as follows:

$$R = \frac{\sum_{i=1}^{N}\left(X_{O_i} - \overline{X_O}\right)\left(X_{R_i} - \overline{X_R}\right)}{\sqrt{\sum_{i=1}^{N}(X_{O_i} - \overline{X_O})^2 \sum_{i=1}^{N}(X_{R_i} - \overline{X_R})^2}} \quad (1)$$

$$RMSE = \sqrt{\frac{1}{2}\sum_{i=1}^{N}(X_{O_i} - X_{R_i})^2} \quad (2)$$

$$MAE = \frac{1}{N}\sum_{i=1}^{N}|X_{O_i} - X_{R_i}| \quad (3)$$

$$Pbias = \frac{\sum(X_{O_i} - X_{R_i})}{\sum X_{O_i}} \quad (4)$$

where N is the number of LST samples, X_{oi} is the i^{th} observed LST value, $\overline{X_O}$ is the average of the observed LST, X_{Ri} is the i^{th} reference LST value, $\overline{X_{R_i}}$ is the average reference LST.

No single metric could capture all of the attributes of the variables. Some are robust with respect to some attributes, whereas they are insensitive to others (Yang et al. 2020; Entekhabi et al. 2010). Previous studies have typically relied on metrics such as r, RMSE, MAE, and Pbias for dataset comparison, recognizing their multiple advantages (Wang et al. 2022; Wen et al. 2022; Liu et al. 2020; Yang et al. 2020; Lee et al. 2013). For instance, Pbias is scale-independent and captures both the magnitude and direction of bias, offering more information than many other metrics. Additionally, MAE is less sensitive to outliers compared to RMSE, making it a more robust choice in cases where extreme values might distort results. Pearson's r, being a standardized measure, allows for easy comparison of relationships between datasets.

2.5 LST Trend Analysis

Trends in daytime and nighttime mean LST of India of all datasets are calculated at seasonal and annual scales for the period 2003–2022 (Fig. 2). The Theil Sen's Slope Estimator and Contextual Mann-Kendall (CMK) significance tests are used to estimate the trend and significance, respectively (Kendall 1975; Sen 1968; Theil 1950). The Theil-Sen slope (TSS) estimator, offers a non-parametric method for estimating trends in time series data (Sen 1968; Theil 1950). It calculates the trend as the median of slopes derived from all pairwise observations, totaling $n(n-1)/2$ calculations. One significant advantage of the TSS method is its robustness against outliers (Rani et al. 2023). Unlike parametric techniques, which can be influenced by extreme values, the TSS estimator can reject up to approximately 29% of wild values without compromising the slope estimate, making it particularly suitable in the present study. The CMK test, a modification of the traditional Mann-Kendall (MK). It

incorporates spatial autocorrelation into the analysis (Neeti and Eastman 2011). By considering the geographical context, the CMK test accounts for spatial autocorrelation by incorporating the spatial relationships between data points into the trend analysis, enhancing the robustness of the trend detection in spatial data. In the trend analysis, the present study averaged monthly LST values to seasonal scales and then estimated trends for each season separately. This approach retains the seasonal components by examining each season independently, rather than entirely removing or deseasonalizing them. Consequently, the analysis captures any distinct trends within each season, providing insights into how LST changes occur across different times of the year.

2.6 Classification of Climatic Regions of India

India, situated in South Asia, occupies a landmass spanning approximately 3.2 million km^2 (Fig. 1). Its diverse topography encompasses everything from mountains and plains to deserts and coastal areas, contributing to its rich natural heritage and cultural tapestry (Fig. 1). For analysis of LST, India has been categorized into six climatic regions, determined by its geographical, topographical, and climatological homogeneity (Dimri 2019; Pal and Al-Tabba 2010) (Fig. 1). These regions include (i) Hilly Regions (HR), (ii) Northwest (NW), (iii) Central Northeast (CNE), (iv) Northeast (NE), (v) West Central (WC), and (vi) Peninsular (P) (Fig. 1).

Besides physiography, the LULC data for the year 2022 is derived from the combined Terra and Aqua MODIS Land Cover Type MCD12Q1 v6.1 dataset, available at 500 m spatial resolution (Friedl and Sulla-Menashe 2022). The characteristics of land use and land cover (LULC) are shown as it is the main determinants of LST conditions in an area. The present study has used the Food and Agricultural Organization (FAO) Land Cover Classification System (LCCS2) and merged the eleven LULC classes into six major classes (Fig. 1). Around 68% of the total area of India is under the herbaceous/croplands, whereas forest and barren occupy about 28% (Fig. 1). Urban and built-up lands, permanent snow and ice, and water bodies together cover less than 5% of the total area. The prevalence of cropland and vegetation highlights them as the most dominant land cover types, which can significantly influence LST in the high-elevated regions of the study area (e.g., HR). Additionally, the area under barren land can impact the LST in the semi-arid and arid parts of the country (e.g., NW) (Fig. 1).

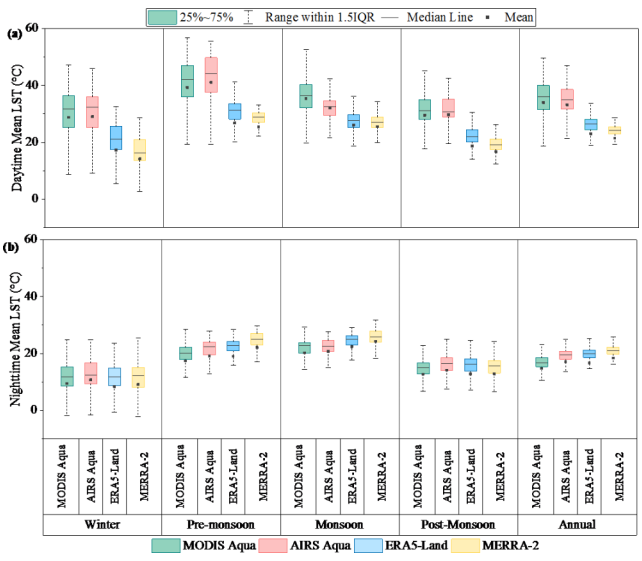

Fig. 3 Distribution of (**a**) daytime and (**b**) nighttime mean LST at seasonal and annual scales across India (2003–2022)

3 Results

3.1 Comparative Daytime and Nighttime Mean LST of Different Datasets

While considering the daytime mean LST of the entire region, it's evident that the highest values occur during the pre-monsoon (33.11 °C), followed by monsoon (29.70 °C), post-monsoon (23.64 °C), and winter (22.28 °C) (Fig. 3). Both MODIS and AIRS Aqua exhibit nearly identical daytime mean LST values across the respective time scales (Fig. 3a). The daytime mean LST of satellite datasets reaches approximately 40 °C in pre-monsoon, (MODIS: 39.26 °C; AIRS: 41.05 °C), 33 °C during the monsoon (MODIS: 35.30 °C; AIRS: 31.99 °C), 29 °C in post-monsoon (MODIS: 29.51 °C; AIRS: 29.68 °C), and 29 °C in winter (MODIS: 28.73 °C; AIRS: 28.97 °C) (Fig. 3a). Overall, the annual daytime mean LST is 33.99 °C from MODIS and 33.17 °C from AIRS. Similar to the satellite datasets, both reanalysis datasets also exhibit comparable values in their respective seasons (Fig. 3a). From reanalysis, the daytime mean LST registers around 26 °C in both pre-monsoon (ERA5-Land: 26.80 °C; MERRA-2: 25.34 °C) and monsoon (ERA5-Land: 26.01 °C; MERRA-2: 25.50 °C) (Fig. 3a). Additionally, daytime mean LST is close to 17 °C in post monsoon (ERA5-Land: 18.68 °C; MERRA-2: 16.68 °C), and around 15 °C in winter (ERA5-Land: 17.28 °C; MERRA-2: 14.14 °C) (Fig. 3a). On an annual scale, the ERA5-Land and MERRA-2 show a daytime mean LST of 23.02 °C and 21.41 °C, respectively (Fig. 3a). Comparing the daytime mean LST of satellite datasets, AIRS tends to show slightly higher values than MODIS in all seasons except during the monsoon. However, on an annual scale, MODIS reports slightly higher daytime mean LST than AIRS. In the reanalysis datasets, ERA5-Land consistently

records higher daytime mean LST than MERRA-2 across all time scales. In both seasonal and annual contexts, the satellite datasets have consistently documented higher daytime mean LST compared to the respective reanalysis datasets, which could be attributed to differences in their spatial resolution and method of data collection (Mal et al. 2022).

Unlike daytime observations, all four datasets indicate the highest nighttime mean LST values during the monsoon (22.03 °C), followed by pre-monsoon (19.56 °C), post-monsoon (13.27 °C), and winter (9.59 °C) (Fig. 3b). In nighttime mean LST, both satellite and reanalysis datasets register nearly identical values across all time scales (Fig. 3b). Across India, the nighttime mean LST is about 22 °C during monsoon (range- MODIS: 20.36 °C; MERRA-2: 24.43 °C), 19 °C in pre-monsoon (range- MODIS: 17.60 °C; MERRA-2: 22.36 °C), 13 °C during post-monsoon (range- ERA5-Land: 12.78 °C; AIRS: 14.36 °C), and 9 °C in winter (range- ERA5-Land: 8.34 °C; AIRS: 10.95 °C) (Fig. 3b). Additionally, the annual nighttime mean LST values are 14.92 °C, 16.71 °C, 17.21 °C, and 18.63 °C for MODIS, ERA5-Land, AIRS, and MERRA-2, respectively (Fig. 3b). Between satellite datasets, AIRS has recorded higher nighttime mean LST values than MODIS at seasonal and annual scales. In the reanalysis, the nighttime mean LST observations from MERRA-2 are slightly higher than those from ERA5-Land across all time scales. Comparing satellite and reanalysis nighttime mean LST, the reanalysis datasets have slightly higher values than satellite ones during pre-monsoon and monsoon seasons. However, winter and post-monsoon satellite datasets registered slightly higher values than those of reanalysis. Overall, on an annual scale, the nighttime mean LST is higher in reanalysis than the satellite observation.

The present study observed that in both satellite and reanalysis datasets, the daytime mean LST is significantly higher than the nighttime mean LST at both seasonal and annual scales (Fig. 3). In satellite datasets, there is an average difference of about 17 °C between daytime and nighttime mean LST, whereas, the difference between the reanalysis daytime and nighttime mean LST is 5 °C only. This could be attributed to the fact that satellite data provides finer spatial and temporal resolution, capturing more detailed daytime LST variations, while reanalysis data is more generalized (Wan 1999,2019; Bosilovich et al. 2015; Tian et al. 2020; Thrastarson et al. 2020, 2021; Muñoz-Sabater et al. 2021). Satellites directly measure LST, leading to more extreme daytime measurements, whereas reanalysis models smooth out variations. Another possible reason could be atmospheric conditions which affect satellite data, contributing to the higher observed daytime LST compared to reanalysis data.

In both daytime and nighttime, India has experienced the highest LST in pre-monsoon and monsoon seasons due to several reasons like vertical rays of the sun on the Tropic of Cancer, increasing cloud cover, higher humidity level, reduced evaporative cooling, etc. (Linacre and Geerts 1997). The difference in LST between daytime and nighttime is primarily due to differences in solar radiation and heat transfer processes (Linacre and Geerts 1997). The present study identified pre-monsoon as the warmest season followed by monsoon in daytime mean LST, whereas, monsoon is the warmest one in nighttime mean LST, with pre-monsoon following closely behind. Meanwhile, winter remained the coldest season, with post-monsoon trailing behind for both daytime and nighttime mean LST. These results are in line with previous studies conducted across different parts of India and its surrounding regions (Mal et al. 2022, 2023; Prakash and Norouzi 2020).

3.2 Comparison Evaluation of Daytime and Nighttime Mean LST of Different Datasets

The comparison of satellite and reanalysis datasets of daytime and nighttime mean LST over India (2003–2022) are also studied to understand the associations among the datasets (Table 2). Overall, very high correlation coefficients (>0.9) are found among all the datasets (except MODIS Aqua and MERRA-2 during at annual scale: $r=0.87$), indicating the close association of the datasets (Table 2). On an annual scale, the satellite datasets exhibit RMSE values higher by 0.47 °C during the daytime and 0.61 °C during the nighttime compared to the reanalysis values (Table 2). In the case of daytime mean LST, the MAE for satellite datasets is 2.51 °C, which is lower than the value of reanalysis datasets (2.74 °C) (Table 2). While in nighttime mean LST, the MAE value of satellite datasets is 1.05 °C higher than that of reanalysis (1.71 °C) (Table 2). Additionally, the Pbias values of satellite datasets are −2.51% during daytime mean LST and 15.50% during nighttime, indicating the underestimation and overestimation of LST on average, respectively (Table 2). In contrast, the reanalysis datasets suggest a significant overestimation during daytime (9%) and an underestimation during nighttime (−8.70%) (Table 2). Overall, the daytime mean LST of India obtained from satellite datasets shows higher values in comparison to reanalysis data. Nevertheless, the mean LST during nighttime of satellite data is close to reanalysis data. This synchronization highlights the consistency in nighttime LST across all datasets compared to daytime observations. Essentially, giving precedence to nighttime LST data over daytime data improves the quality of results. The noticeable differences among all four datasets may be attributed to their utilization of different algorithms and modeling techniques in data generation

Table 2 Inter-dataset (MODIS Aqua, AIRS Aqua, ERA5-Land, and MERRA-2) comparison of daytime and nighttime mean LST of India for the period 2003–2022

Time scales /indicators	Daytime						Nighttime					
	MODIS Aqua vs. AIRS Aqua	MODIS Aqua vs. ERA5-Land	MODIS Aqua vs. MERRA-2	AIRS Aqua vs. ERA5-Land	AIRS Aqua vs. MERRA-2	ERA5 Land vs. MERRA-2	MODIS Aqua vs. AIRS Aqua	MODIS Aqua vs. ERA5-Land	MODIS Aqua vs. MERRA-2	AIRS Aqua vs. ERA5-Land	AIRS Aqua vs. MERRA-2	ERA-5Land vs. MERRA-2
Winter												
r	0.96	0.95	0.93	0.96	0.96	0.99	0.97	0.97	0.96	0.98	0.98	0.98
RMSE (°C)	3.6	12.03	15.29	12	15.21	5	3.02	3.39	3.15	4.27	3.22	2.54
Pbias (%)	0.80	−39.10	−51.30	65.50	106.60	25.70	14.10	−10.20	−3.10	26.90	17.60	−7.00
MAE (°C)	2.45	11.09	14.6	11.33	14.78	4.66	1.98	1.99	1.84	2.48	2.11	1.56
Pre-monsoon												
r	0.94	0.92	0.93	0.95	0.93	0.98	0.96	0.96	0.94	0.97	0.96	0.99
RMSE (°C)	4.62	13.23	15.29	14.56	16.36	4.05	3.09	3.86	5.85	3.11	4	3.9
Pbias (%)	4.40	−31.30	−51.30	52.00	62.30	7.10	9.70	9.90	27.40	−0.20	−13.80	−13.80
MAE (°C)	3.44	12.2	14.6	13.94	15.62	3.23	2.37	3.06	5.18	2.06	3.34	3.07
Monsoon												
r	0.94	0.92	0.93	0.95	0.93	0.98	0.94	0.96	0.94	0.96	0.96	0.98
RMSE (°C)	4.62	13.23	15.29	14.56	16.36	4.05	2.51	3.22	4.85	2.93	3.98	2.72
Pbias (%)	4.40	−31.30	−51.30	52.00	62.30	7.10	2.70	11.20	20.20	−7.60	−14.50	−7.50
MAE (°C)	3.44	12.2	14.6	13.94	15.62	3.23	1.65	2.72	4.21	2.3	3.54	1.91
Post-monsoon												
r	0.94	0.92	0.87	0.95	0.92	0.98	0.94	0.96	0.95	0.98	0.98	0.99
RMSE (°C)	3.29	11.59	13.67	11.47	13.49	3.97	2.91	3.65	3.22	2.59	2.59	2.46
Pbias (%)	0.5	−36.10	−43.90	57.30	78.80	14.30	11.7	1.80	1.50	10.00	10.00	0.50
MAE (°C)	2.13	10.56	12.86	10.72	12.96	3.36	2.15	2.33	1.99	1.81	1.81	1.54
Annual												
r	0.93	0.9	0.87	0.95	0.93	0.98	0.96	0.96	0.94	0.98	0.97	0.99
RMSE (°C)	3.72	11.77	13.51	10.57	12.19	3.25	3.32	3.96	4.78	2.88	2.45	2.71
Pbias (%)	−2.50	−31.80	−37.30	43.00	55.40	9.00	15.50	14.10	25.00	1.20	28.20	−8.70
MAE (°C)	2.51	10.76	12.64	9.91	11.74	2.74	2.76	3.31	4.23	1.64	1.89	1.71

Note: Correlation coefficient (r), root mean square error (RMSE), percentage bias (Pbias), and mean absolute error (MAE).

Remarks:

• High correlations among the datasets suggest their suitability for tracking relative LST variations in a region and useful for monitoring land atmosphere feedback mechanism.

• High RMSE in MODIS Aqua vs. ERA5-Land/MERRA-2 comparisons (especially daytime) may limit MODIS's precision for applications requiring exact temperatures, like agriculture and short-term forecasts.

• Significant biases highlight the need for correction in applications such as drought and climate modeling, enhancing accuracy by aligning data with observed values.

• Lower MAE for nighttime data suggests these datasets are dependable for applications like urban heat island (UHI) studies, benefiting from stable error levels.

• MODIS Aqua- Micro level -urban heat islands, monitoring vegetation health, identifying heat stress, and assessing drought conditions

• AIRS Aqua & MERRA-2- regional studies related to vegetation health and climate modelling

• ERA5-Land- climate monitoring, and ecosystem modelling at finer spatial scale

(Wang et al. 2022; Liu et al. 2020). Moreover, the variations are relatively high between satellite (only in cloud-free conditions) and reanalysis datasets (in all conditions) (Wang et al. 2022; Liu et al. 2020). All these differences are reflected in the mean LST values between the four datasets in the present study as well.

3.3 Spatial Distribution of Daytime and Nighttime Mean LST

Across India, the regions of NW, WC, and P (encompassing the Thar desert and Deccan plateau) consistently exhibit the highest daytime mean LST in all the seasons (Fig. 4). Conversely, LST remains moderate over the northern NW, CNE, and NE (including the Indo-Gangetic-Brahmaputra plain), and lowest over the HR (Himalaya) (Fig. 4). Among the six climatic regions, WC and P (parts located on the eastern side of the Western Ghats) experience the highest daytime mean LST during winter (satellite: 30 °C to > 45 °C; reanalysis: 15 °C to 30 °C), while the HR region recording the lowest values (satellite: −30 °C to 15 °C; reanalysis: < −30 °C to 15 °C) (Fig. 4a, f, k, p). In the pre-monsoon period, except for HR (< 15 °C), the entire country experiences daytime mean LST of > 30 °C (some parts of NW and WC: >45 °C) based on satellite data (Fig. 4b, g). However, in reanalysis data, daytime mean LST values varied between 15 °C and 45 °C across the country (except HR: < 0 °C) during pre-monsoon (Fig. 4l, q). During monsoon season, according to satellite data, the entire country experiences daytime mean LST between 15 °C and 45 °C, except for the Thar desert (> 45 °C) (Fig. 4c, h). However, reanalysis data show a variation from − 15 °C to 45 °C only across the study area (Fig. 4m, r). In the post-monsoon period, NW, WC, and P experience daytime mean LST between 30 °C and 45 °C based on satellite data, while reanalysis data show a range of 15 °C to 30 °C (Fig. 4d, i, n, s). Conversely, CNE, NE, and HR record temperatures between − 15 °C and 30 °C according to satellite data, and < −30 °C to 15 °C according to reanalysis datasets (Fig. 4d, i, n, s). Overall, the observations from satellite datasets at an annual scale vary from − 15 °C to > 45 °C (parts of NW, WC, and P: >45 °C; HR: < 15 °C), whereas in reanalysis, the values lie below 30 °C across the study area (except Thar desert: > 30 °C) (Fig. 4e, j, o, t).

Unlike daytime mean LST, nighttime mean LST of both satellite and reanalysis data are largely consistent within their respective climatic regions, (Fig. 5). During winter, nighttime mean LST is relatively high (> 15 °C) in regions such as P, WC, southern NW, and eastern CNE, while it is lower (< 15 °C) in the rest of the study area across all datasets (Fig. 5a, f, k, p). In the pre-monsoon season, all datasets record nighttime mean LST between 15 °C and 30 °C across WC, P, NW, CNE, and NE (Fig. 5b, j, l, q). However, in HR, the range of pre-monsoon nighttime mean LST (−30 °C to 15 °C) is consistent across both datasets (Fig. 5b, j, l, q). Similarly, during the monsoon season, except HR (−15 °C to 15 °C), all regions experience nighttime mean LST of 15 °C to 30 °C according to all datasets (Fig. 5c, h, m, r). However, in other parts of NW, monsoon nighttime mean LST goes above 30 °C from MERRA-2 (Fig. 5c, h, m, r). Furthermore, in the post-monsoon period, nighttime mean LST ranges between 0 °C and 30 °C in all climatic regions except HR (< 0 °C) across all datasets (Fig. 5d, i, n, s). Annually, HR consistently experiences the lowest nighttime mean LST (< 15 °C) through both satellite and reanalysis datasets, while over other climatic regions, it ranges between 15 and 30 °C in both satellite and reanalysis datasets (Fig. 5e, j, o, t).

The mean LST conditions of the present study align closely with the other studies covering the different parts of India and neighboring regions (Mal et al. 2022, 2023; Wang et al. 2022; Prakash and Norouzi 2020). The spatial variations in daytime and nighttime mean LST are mainly influenced due to the physiography and LULC of the regions (Prakash and Norouzi 2020; Khandan et al. 2018; Mal et al. 2022; Chaudhuri and Mishra 2016; Singh et al. 2024; Mukherjee and Singh 2020). The elevated regions of the HR (dense vegetation) exhibit the lowest mean LST, while the semi-arid and arid regions (sparse vegetation) of India, such as the Thar Desert and the Deccan Plateau, register the highest mean LST in both daytime and nighttime. In the NE region, the eastern part, characterized by hills (dense vegetation and low urban growth), generally shows lower mean LST (both daytime and nighttime) compared to its western plains (Figs. 1, 4 and 5). The influence of urbanization on mean LST, particularly in the form of Urban Heat Island (UHI) effects, has been well-documented across various Indian cities over the past two decades (Naikoo et al. 2022; Shahfahad et al. 2021; Siddiqui et al. 2021; Sultana and Satyanarayana 2018). These studies have highlighted the significant impact of land-use changes, including urbanization and deforestation, on UHI dynamics in several cities and other metropolitan regions.

3.4 Temporal Variability of Daytime and Nighttime LST

Over 20 years, there are noticeable variations in the annual daytime and nighttime mean LST across all datasets (Fig. 6). Regarding daytime mean LST, all four datasets display a similar pattern over the period, albeit with variances in the mean values (Fig. 6a). Notably, the highest daytime mean LST across all datasets occurred in 2009 (MODIS: 34.74 °C; AIRS: 34.05 °C; ERA5-Land: 23.62 °C;

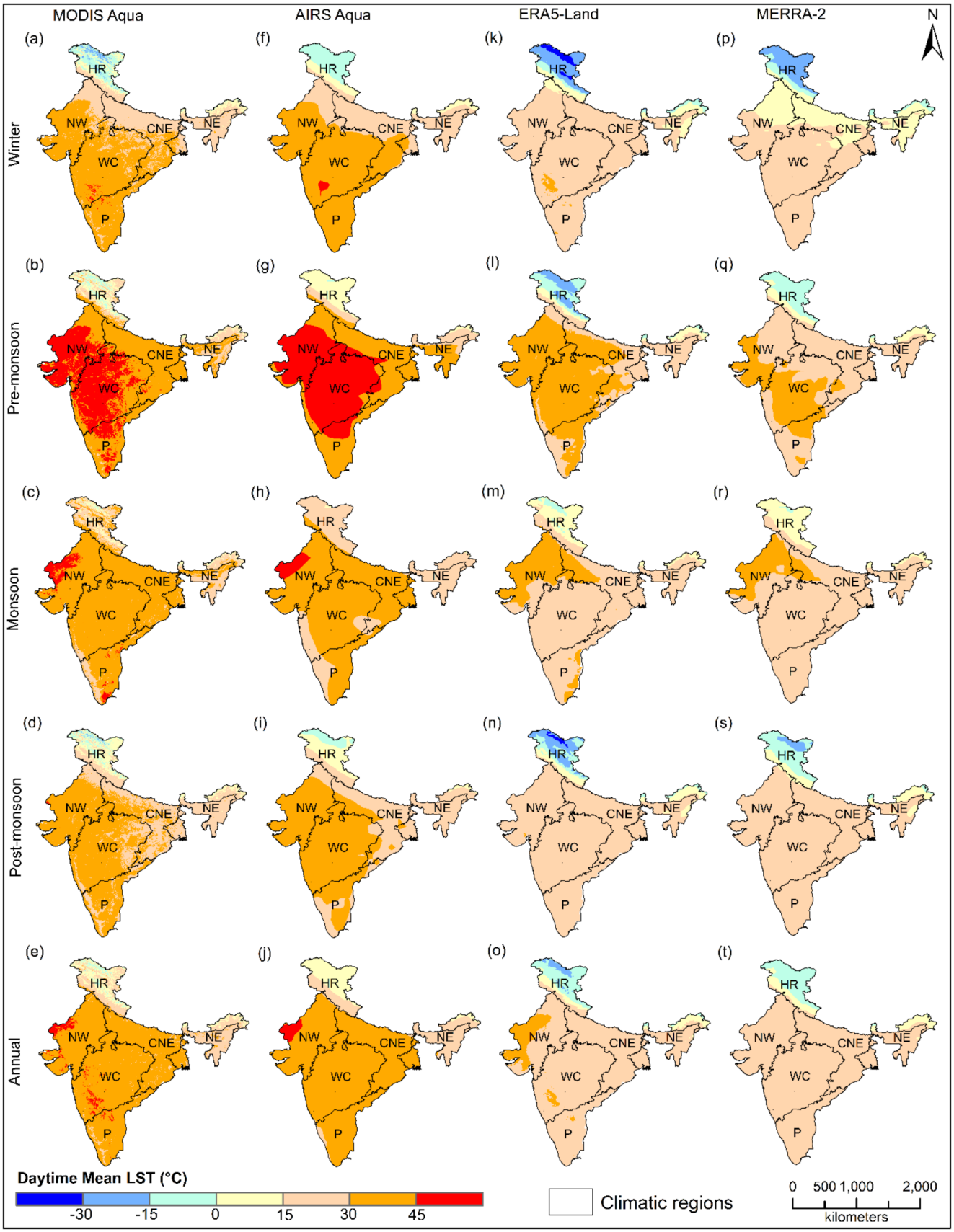

Fig. 4 Spatial distribution of daytime mean LST at seasonal and annual scales across India (2003–2022)

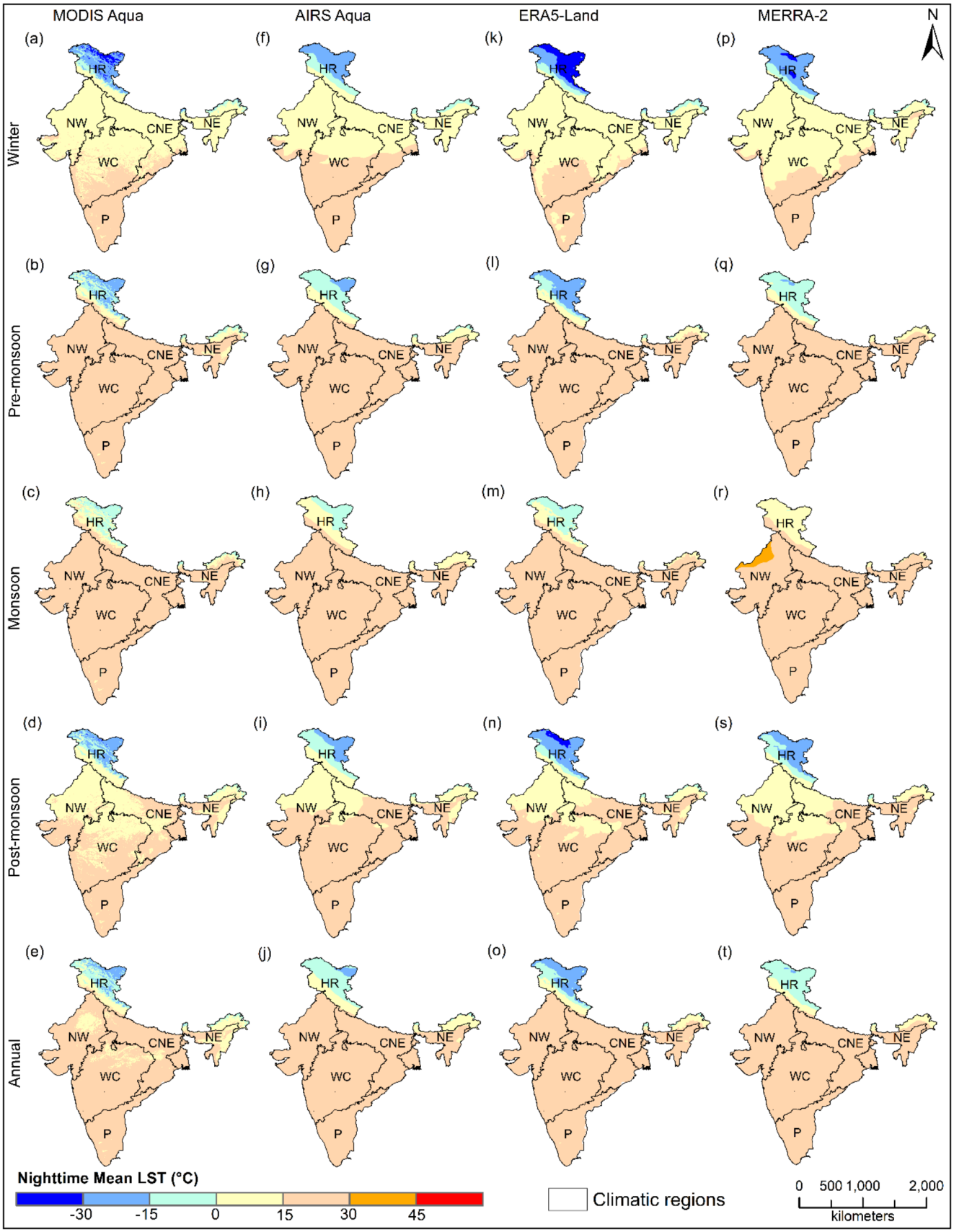

Fig. 5 Spatial distribution of nighttime mean LST at seasonal and annual scales across India (2003–2022)

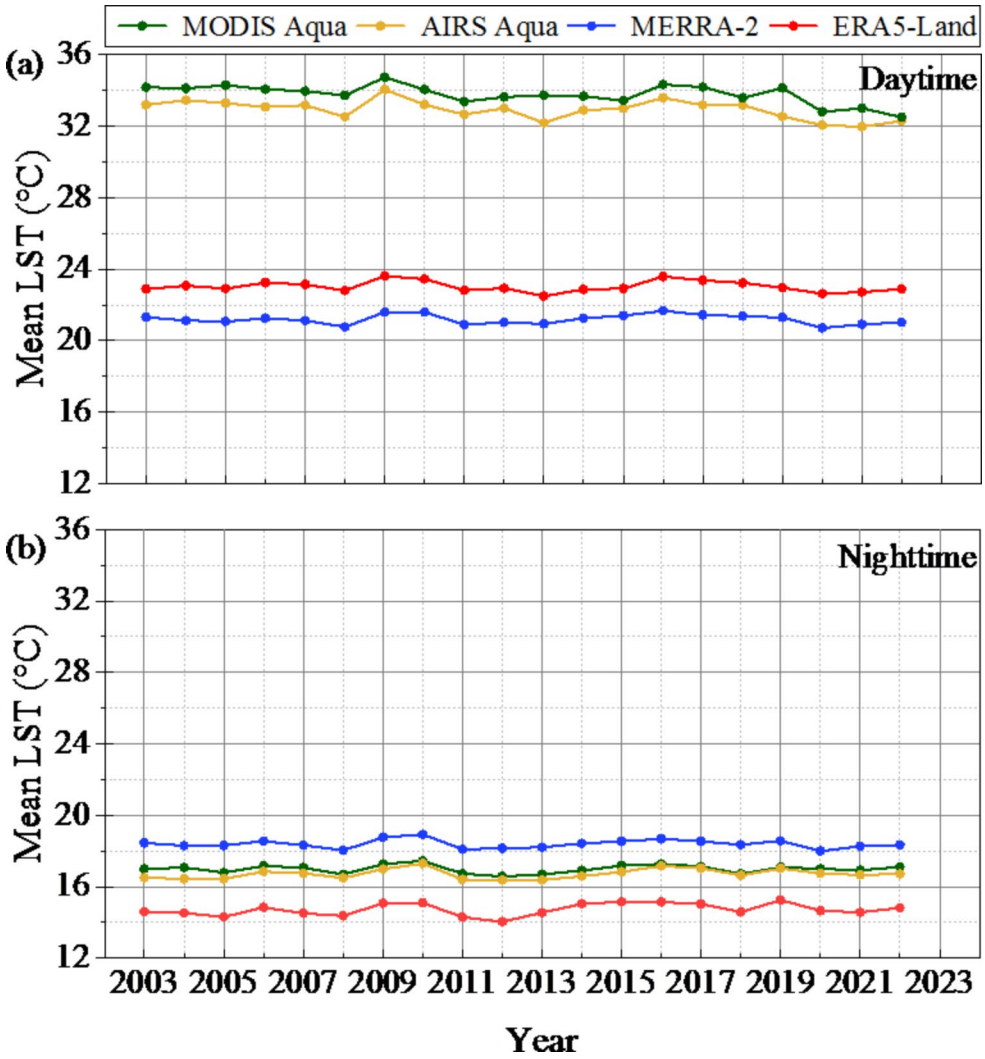

Fig. 6 Temporal variations in daytime and nighttime annual mean LST of India from 2003 to 2022 from MODIS Aqua, AIRS Aqua, ERA5-Land, and MERRA-2. Note: Significant El Niño events in 2009-10 and 2015-16, and marked by major drought occurrences over India in 2009 and 2015

MERRA-2: 21.59 °C), followed by subsequent years mostly recording values below the 20-year average (Fig. 6a). Similarly, a comparable pattern emerges in nighttime mean LST across the four datasets (Fig. 6b). Furthermore, the analysis indicates that daytime mean LST values from satellite datasets consistently surpass those from the reanalysis dataset throughout the entire period (Fig. 6a, b). Conversely, nighttime LST variations between datasets are relatively minimal (Fig. 6a, b). Additionally, the interannual variations of the all-India mean LST from 2003 to 2022 identified 2009 as the warmest year in the daytime, with 2016 following closely. Conversely, for the nighttime mean LST, the warmest years were 2010 followed by 2016. This same year was identified as the warmest in India (Prakash and Norouzi 2020), as well as on a global scale (Susskind et al. 2019). The inter-annual variability found in LSTs during the years 2009 and 2016 can be attributed to large-scale climatic events. Specifically, the year 2009 was characterized by an El Niño event, which is often associated with higher-than-average temperatures in many regions, including India (Null 2024; Choudhury 2024; Rao et al. 2021; Mishra 2020). Similarly, 2016 experienced one of the strongest El Niño events on record, likely contributing to the elevated LSTs observed during that year. In contrast, La Niña conditions are generally linked to cooler temperatures (Null 2024). Additionally, regional factors, such as monsoon variability, significantly influence these temperature extremes; weaker or delayed monsoons can result in higher LSTs, whereas robust monsoon seasons typically lead to cooler surface temperatures. Throughout the study duration, the occurrence of years with values above and below the mean is roughly equal, making it inconclusive to determine whether the region is experiencing cooling or warming trends considering the regional annual mean. Therefore, the spatial distribution of trends in daytime and nighttime mean LST is analyzed for better understanding.

3.5 Comparison of Trends in Daytime and Nighttime LST of Different Datasets

All datasets show an average cooling trend in daytime (range: −0.024 to −0.133 °C/yr), and mixed trends in nighttime (range: −0.081 to 0.055 °C/yr) mean LST of India at seasonal and annual scales during the study period (Fig. 7a, b). Trends in daytime mean LST of India show high variations among the different datasets compared to nighttime LST across seasons (Fig. 7a, b). In winter, the average significant change rate of daytime mean LST (−0.133 °C/yr) derived from MODIS Aqua, AIRS Aqua, ERA5-Land, and MERRA-2 was approximately −0.190, −0.176, −0.088, and −0.080 °C/yr, respectively (Fig. 7a). Additionally, during the pre-monsoon period, the trend from satellite data ranges from −0.139 (MODIS Aqua) to −0.086 °C/yr (AIRS Aqua), while in the reanalysis, it varies from −0.022 °C/yr (MERRA-2) to 0.152 (ERA5-Land) (Fig. 7a). During monsoon, the satellite data shows cooling trend in daytime mean LST (MODIS Aqua: −0.142 °C/yr and AIRS Aqua: −0.081 °C/yr), while reanalysis shows warming trends (ERA5-Land: 0.017 °C/yr and MERRA-2: 0.002 °C/yr) (Fig. 7a). During post-monsoon, except MERRA-2 (−0.031 °C/yr), all three datasets show cooling trend with highest in AIRS Aqua (−0.139 °C/yr), followed by MODIS Aqua (−0.105 °C/yr), and ERA5-Land (−0.036 °C/yr) in daytime mean LST (Fig. 7a). The annual daytime LST trend over the past 20 years reveals distinct variations among different datasets. ERA5-Land shows a slight warming trend of 0.003 °C/yr, while the other datasets indicate cooling trends: MERRA-2 at −0.004 °C/yr, AIRS Aqua at −0.091 °C/yr, and MODIS Aqua at −0.115 °C/yr (Fig. 7a).

Nighttime mean LST shows the highest cooling trend through ERA5-Land (−0.152 °C/yr), followed by MERRA-2 (−0.141 °C/yr), and AIRS Aqua (−0.067 °C/yr), while MODIS Aqua (0.037 °C/yr) shows warming trend in the winter season (Fig. 7b). In pre-monsoon, MODIS Aqua (0.068 °C/yr), AIRS Aqua (0.004 °C/yr), and ERA5-Land (0.020 °C/yr) show warming trend, while MERRA-2 with a rate of change of −0.022 is observed a cooling trend (Fig. 7b). During monsoon, the highest nighttime mean LST trend is recorded in MODIS Aqua (0.072 °C/yr), followed by ERA5-Land (0.037 °C/yr), MERRA-2 (−0.022 °C/yr), and AIRS Aqua (−0.030 °C/yr) (Fig. 7b). In post-monsoon nighttime LST, all the datasets show warming trend, with the highest in MODIS Aqua (0.067 °C/yr), MERRA-2 (0.061 °C/yr), ERA5-Land (0.050 °C/yr), and AIRS Aqua (0.043 °C/yr) (Fig. 7b). Over 20 years, the annual nighttime LST shows a significant warming trend of 0.011 °C/yr, 0.031 °C/yr, and 0.049 °C/yr from AIRS Aqua, ERA5-Land, and MODIA Aqua respectively, while MERRA-2 shows the slight cooling trend (−0.002 °C/yr) (Fig. 7b). Overall, the daytime mean LST of satellite datasets shows a cooling trend, while reanalysis show warming (except winter), in all time scales (Fig. 7a). However, nighttime mean LST shows consistency in trends between satellite and reanalysis datasets in all the seasons except pre-monsoon (Fig. 7b). The divergence observed between daytime and nighttime LST trends can be significantly influenced by atmospheric processes, including boundary layer dynamics and aerosol concentrations. During daylight hours, solar radiation heats the surface, and fluctuations in boundary layer thickness can lead to increased variability in daytime LST. Furthermore, aerosols, which are typically more concentrated during the day due to anthropogenic activities, can impact the absorption and scattering of solar radiation, thereby contributing to differences in daytime LST trends. Conversely, nighttime LST is predominantly influenced by radiative cooling and is less affected by the processes occurring during the day.

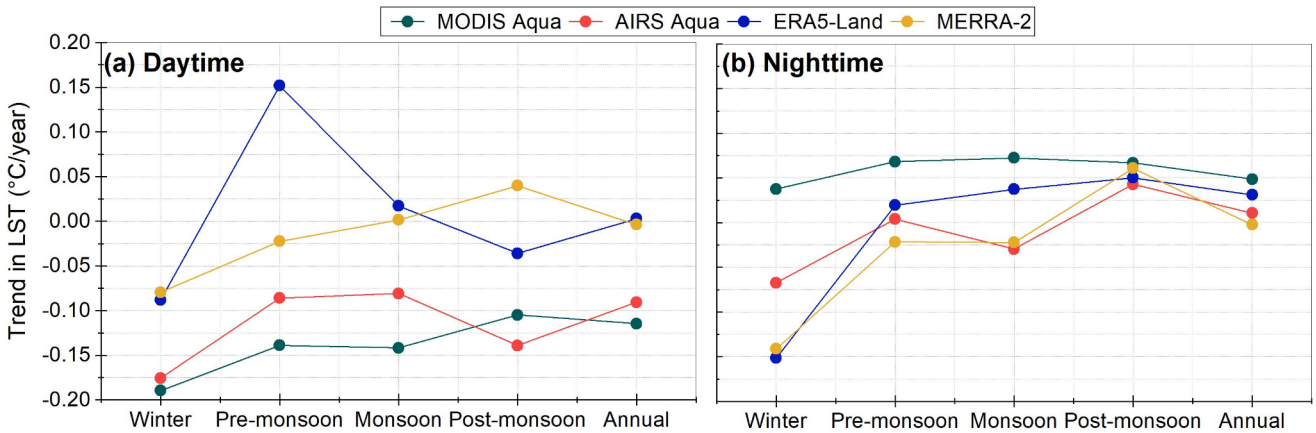

Fig. 7 Distribution of (**a**) daytime and (**b**) nighttime LST trends at seasonal and annual scales across India (2003–2022) (all values are significant at 0.1 level)

3.6 Spatial Distribution of Seasonal/annual Trends in Daytime and Nighttime LST

Almost all climate regions of India have been exhibiting cooling trends in daytime mean LST across all seasons (Fig. 8). During winter, distinctive cooling trends in daytime mean LST are observed across all climatic regions in the datasets (Fig. 8a, f, k, p). However, notable divergence is detected in parts of NW and NE, where all datasets indicate slight warming trends (range: 0 to 0.5 °C/yr) (Fig. 8a, f, k, p). Pre-monsoon trends in daytime mean LST from satellite data indicate cooling across all regions (except a few patches in NW, HR, and P), while reanalysis data indicates cooling (0 to −0.5 °C/yr) only in CNE, and few patches of NW, WC, NE, and P (Fig. 8b, g, l, q). During the monsoon season, both cooling and warming trends are observed in daytime mean LST across all datasets, with MODIS showing cooling in all climatic regions, whereas AIRS indicates warming (0 to 0.5 °C/yr) in HR and certain patches of CNE and NE (Fig. 8c, h). Reanalysis data also depict a mix of cooling and warming trends in daytime mean LST in specific patches of NW, CNE, and WC during the monsoon (Fig. 8m, r). Post-monsoon analysis reveals a cooling trend (0 to −0.5 °C/yr) in daytime mean LST across all regions (except eastern CNE, NE, and eastern HR) in satellite datasets (Fig. 8d, i). Furthermore, both reanalysis datasets in the same season exhibit a similar distribution in daytime mean LST trend (0 to 0.5 °C/yr: P, WC, CNE, and NE; 0 to −0.5: NW and HR) (Fig. 8n, s). Overall, daytime mean LST trends during winter appear more consistent (with wider coverage) across all datasets compared to other seasons (Fig. 8). At an annual scale, satellite data consistently show cooling trends in daytime mean LST across almost all climate regions of India, whereas reanalysis data indicate both cooling and warming trends (Fig. 8e, j, o, t). Additionally, satellite datasets have a more significant trend area than the reanalysis datasets.

During the nighttime, the rate of change in mean LST ranges between − 1 °C/yr and 0.5 °C/yr across all the datasets (Fig. 9). In winter, the nighttime mean LST from satellite datasets shows a similar trend distribution, although there is variation in their trend values (Fig. 9a, f). Across all climatic regions, the winter nighttime mean LST shows a similar trend (−0.5 °C/yr to 0.5 °C/yr) from all datasets, except HR from MERRA-2 (0 to −1 °C/yr) (Fig. 9p). During pre-monsoon, NW shows a warming trend (0 to 0.5 °C/yr) in all datasets. MODIS Aqua shows a warming trend across all regions, whereas AIRS Aqua highlights cooling in HR, WC, P, and NE (Fig. 9b, g). In contrast, both reanalysis observed an almost similar rate of change (−0.5 to 0.5 °C/yr) and also covered nearly the same spatial distribution (Fig. 9l, q). During the monsoon season, MODIS Aqua and ERA5-Land data reveal a predominantly warming trend (0 to 0.5 °C/yr) in nighttime mean LST over most of India, except in the WC (Fig. 9c, m). Conversely, AIRS Aqua and MERRA-2 show a cooling trend (0 to −0.5 °C/yr) across large parts of the study area (Fig. 9h, r). In the post-monsoon, all four datasets have shown nearly a similar rate of change (0 to 0.5 °C/yr) and the same spatial distribution in nighttime mean LST (Fig. 9d, i, n, s). Additionally, all datasets show a cooling trend (~ −0.5 °C/yr) over the same regions (Fig. 9d, i, n, s). On an annual scale, all climate regions show variations in trend values through different datasets (Fig. 9c, j, o, t). For example, across HR, MODIS Aqua and ERA5-Land show a warming trend in most of the area, while a cooling trend from AIRS Aqua and MERRA-2 in the region (Fig. 9c, j, o, t). Additionally, NW, WC, CNE, P, and NE show warming trends from all datasets, except AIRS Aqua over WC and P (Fig. 9j) and MERRA-2 over northern NW and CNE (Fig. 9t). Overall, the nighttime mean LST shows a warming trend over the majority of India among all datasets across seasons, indicates the presence of 'nighttime warming effect' (Fig. 9). In contrast, daytime mean LST shows cooling trend among all the datasets across seasons.

4 Discussion

In both seasonal and annual analyses, satellite datasets consistently show higher daytime mean LST compared to reanalysis datasets. This divergence can likely be attributed to disparities in spatial resolution and data collection methodologies between the two sources. When examining nighttime mean LST, reanalysis datasets tend to exhibit slightly high values compared to satellite data, particularly during pre-monsoon and monsoon seasons, possibly due to cloud interference in satellite observations. Conversely, during winter and post-monsoon periods, satellite datasets demonstrate marginally higher values than reanalysis data. On an annual scale, reanalysis datasets consistently portray higher nighttime mean LST compared to satellite observations. The LST estimate disparity between the two datasets has been previously investigated across global and regional levels using various approaches (Wang et al. 2022; Wen et al. 2022; Liu et al. 2020; Retamales-Muñoz et al. 2019; Susskind et al. 2019; Jiménez-Muñoz et al. 2016). The resemblance in the satellite datasets is primarily attributed to the fact that both rely on thermal infrared-based observations and undergo similar retrieval processes (Wang et al. 2022; Liu et al. 2020). Furthermore, they share the same limiting factors, such as providing observations only in cloud-free conditions. Similarly, the results from the two reanalysis datasets exhibit identical absolute values as they are both modeled datasets based on several surface and atmospheric

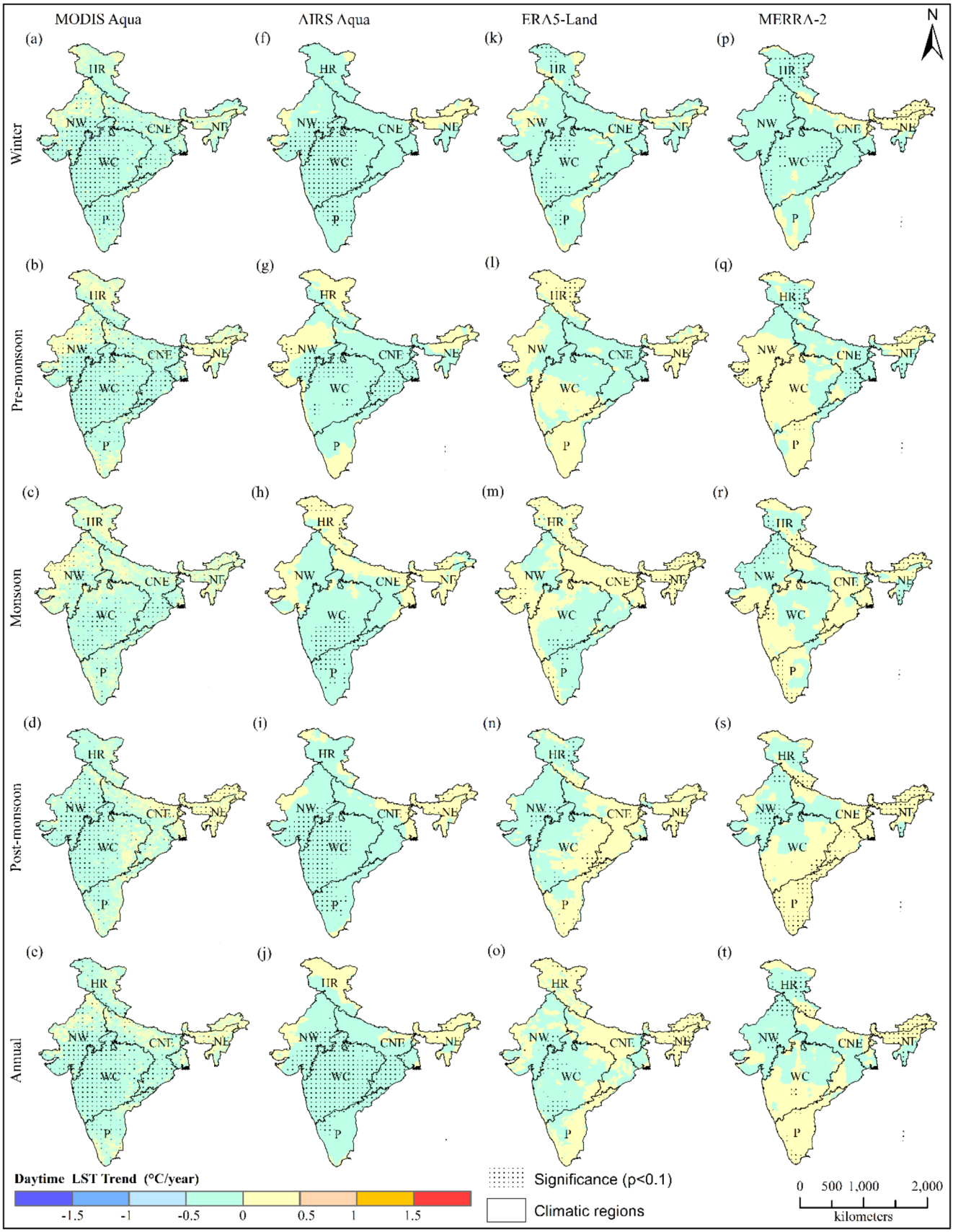

Fig. 8 Spatial variations of daytime LST trend at seasonal and annual scales across India (2003–2022)

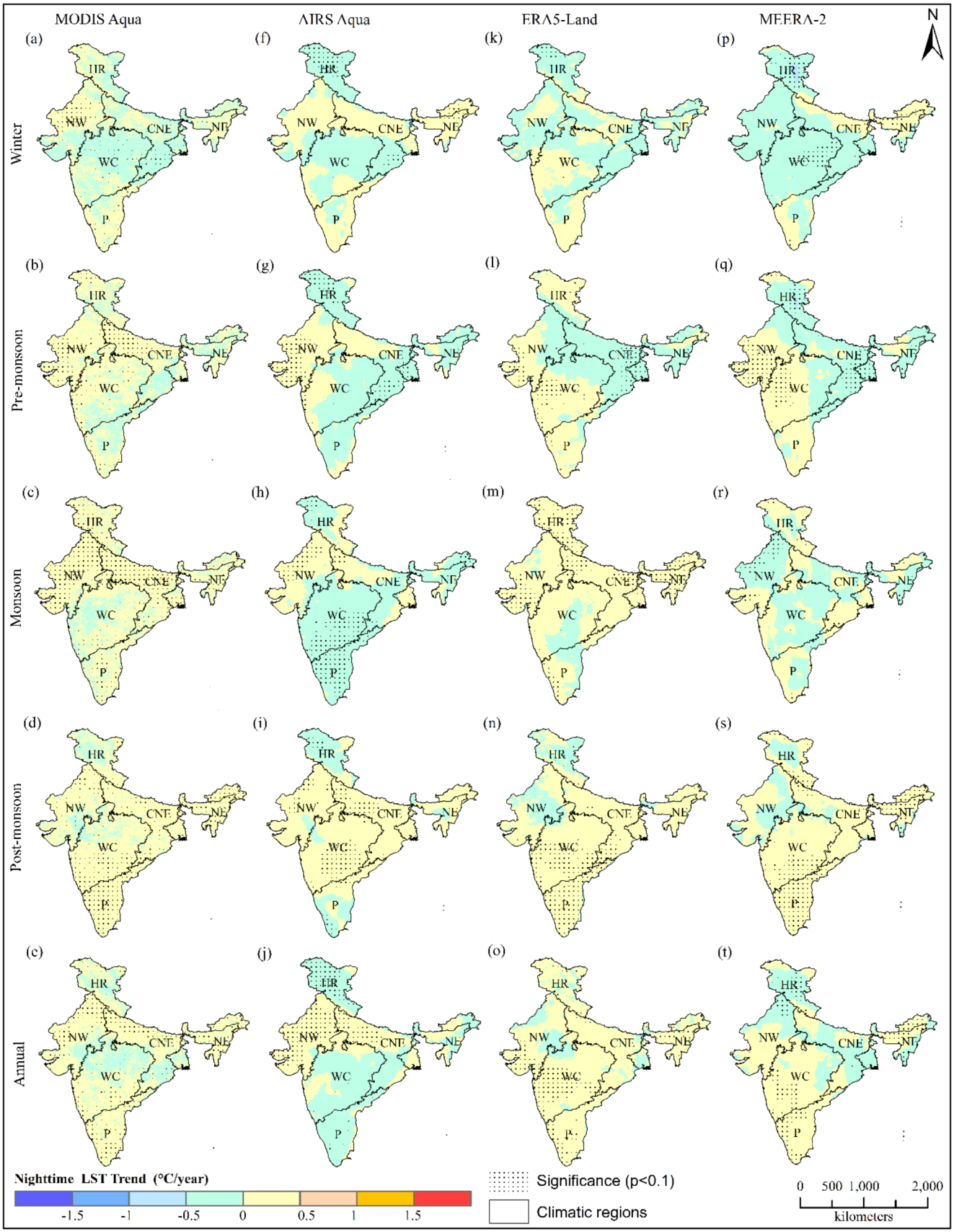

Fig. 9 Spatial variations of nighttime LST trend at seasonal and annual scales across India (2003–2022)

parameters (Wang et al. 2022; Liu et al. 2020; Retamales-Muñoz et al. 2019). However, the present study also reveals noticeable dissimilarities between the LST values (both mean and trend) of the satellite and the reanalysis, possibly due to discrepancies in their data acquisition methods (Li et al. 2023; Zhang et al. 2021). For example, satellite datasets are constrained to cloud-free conditions, whereas ERA5-Land is based on modeled data, potentially contributing to these disparities. These differences may also stem from various other factors, including differences in data resolution, spatial coverage, and the assimilation of ground-based observations (Li et al. 2023; Muñoz-Sabater et al. 2021; Zhang et al. 2021; Zhou and Wang 2016). Comparing these variations between the two types of datasets in daytime and nighttime, it has been found that the differences are more pronounced in the daytime. It may be because of several factors like incoming solar radiation, more pronounced atmospheric conditions (presence of aerosols, water vapor, cloud cover, etc.), surface heating, etc. (Zhang et al. 2021; Liu et al. 2017; Jiménez-Muñoz et al. 2016; Zhou and Wang 2016; Trigo et al. 2008). In contrast, the variation between satellite and reanalysis datasets tends to be lower during nighttime because, at night, atmospheric conditions are generally more stable (Zhang et al. 2021; Liu et al. 2017; Zhou and Wang 2016; Trigo et al. 2008). Nighttime LST offers a more stable and consistent dataset due to minimized external influences, such as solar radiation and human activity, making it particularly valuable for long-term policy development. In the context of urban heat management, nighttime LST can assist in identifying areas that retain heat, thereby contributing to the urban heat island effect. Likewise, in agricultural planning, consistent nighttime temperatures are essential for evaluating plant stress and crop resilience. However, while nighttime LST is a valuable tool, relying exclusively on it may overlook significant diurnal variations, especially in regions with substantial temperature fluctuations between day and night. In such regions, daytime LST may reveal critical insights about temperature extremes, heat exposure, and their effects on human health and agriculture. Therefore, integrating both daytime and nighttime LST data is essential for a more comprehensive understanding and effective policy development, especially in areas with marked diurnal temperature variations.

The present analysis of the annual daytime LST trend over NW, WC, HR, and the western part of CNE is consistent with an earlier study that reported a cooling trend (~2 °C/decade) over western, south-western, and some parts of western Himalaya for the period 2003 to 2017 (Prakash and Norouzi 2020). Furthermore, they have found a warming trend (0 to 0.5 °C/decade) across the northeast and southern parts of the country, which aligns with our trend results over the respective regions (NE and P). The annual nighttime LST trend is consistent with a prior investigation indicating increased LST across much of the country (Prakash and Norouzi 2020). Mal et al. (2022) also found a cooling trend in daytime mean LST at seasonal (except monsoon, MODIS: 0.026 °C/yr; ERA5: 0.017 °C/yr) and annual scales over the Ganga River Basin from 2001 to 2019, using MODIS (winter: −0.078 °C/yr; pre-monsoon: −0.006 °C/yr; post-monsoon: −0.040 °C/yr; annual: −0.017 °C/yr) and ERA5 (winter: −0.020 °C/yr; pre-monsoon: −0.017 °C/yr; post-monsoon: −0.027 °C/yr; annual: −0.017 °C/yr) datasets. Conversely, other studies are showing mixed trends in the different parts of India and neighbouring regions and thus align to some extent with the present study results (Mal et al. 2023; Rani and Mal 2022; Zhao et al. 2019; Vinnarasi et al. 2017). The variances observed can be ascribed to disparities in study parameters such as geographical scope, timeframe (particularly time of 1.30 and 13.30), and data sources. Many of the studies leveraging satellite data predominantly used Terra imagery exclusively or in conjunction with Aqua data. Conversely, evaluation based on reanalysis data commonly relied on daily averages rather than a particular time of the day. The previous studies found LST trend from −3 to 1.5 K/decade and from −3 to 0.5 K/decade at global and India scales, respectively (Sharifnezhadazizi et al. 2019; Liu et al. 2020; Wang et al. 2022). These studies also observed both warming and cooling trends in LST worldwide, consistent with the findings of the present study. The warming trends observed globally are less pronounced over Asia and India, with some data even indicating cooling trends. The contrasting trends between global and Indian land surface temperatures (LST) may suggest complex climate interactions driven by atmospheric circulation patterns, regional human activities, and natural variability. This contrast highlights the importance of regional studies, as global averages can overlook localized effects that are essential for understanding climate impacts on biodiversity, agriculture, and water resources in specific areas.

The present study period shows cooling and warming trends in LST trend which can be attributed to changes in LULC conditions, aerosols concentration, rising precipitable water vapor (PWV), and extreme climatic events (Mal et al. 2022; Null 2024; Rani et al. 2024). The study area experienced a notable LULC change, with cropland expanding significantly by more than 20%, replacing areas primarily classified as barren land, which declined by about 35% during 2005–2023 (National Remote Sensing Centre 2024). In this period, built-up areas also rose by 6.5%, and snow cover increased dramatically by 113.82%. The observed land cover changes might be linked to the contrasting daytime and nighttime LST trends in the region. The expansion of cropland and built-up areas could be contributing to increased heat retention and slower cooling rates at night,

potentially leading to nighttime warming. On the other hand, the increase in snow cover (hilly regions) and the reduction in barren land might support daytime cooling. Snow cover tends to reflect solar radiation, and areas with reduced barren land may absorb less heat compared to other land types. Together, these shifts in land cover may help explain the cooling observed during the day and the warming at night, though other factors could also be at play. Increasing PWV typically lowers daytime LST through cooling effects from cloud cover, though in some cases it may cause slight warming. At night, however, higher PWV more reliably high LST due to stronger greenhouse warming and diminished radiative cooling.

The implications of this study's findings extend to various sectors, including environmental management, urban planning, and climate resilience, highlighting the need for continued refinement and integration of datasets to improve the ability to monitor and mitigate the impacts of changing land surface temperatures in India. For instance, cooling daytime LST may shift plant growth cycles, species distribution, and productivity, while nighttime warming could disrupt ecosystems by altering energy balance. Faster daytime cooling could reduce evapotranspiration and retain soil moisture, benefiting arid regions. It may also help mitigate the Urban Heat Island (UHI) effect, lowering peak temperatures in cities. However, nighttime warming worsens UHI, increasing energy demand, heat stress, and health risks, especially for vulnerable populations. These trends could affect precipitation, humidity, and global energy balance, potentially intensifying heat waves and droughts. Future studies are needed to explore these impacts. The cooling daytime LST is found, especially in the northwest and west-central regions, may suggest regional factors such as increased cloud cover, changes in land use, or human activities that could be offsetting the overall warming trends. Conversely, the rise in nighttime LST across most areas aligns more closely with global warming forecasts, which generally predict higher nighttime temperatures due to the atmosphere's enhanced heat retention. This contrast underscores the diverse impacts of climate change, highlighting that global warming does not uniformly affect all regions. If the cooling trends in daytime LST persist, they could challenge conventional views on climate change effects, warranting further examination of local climate dynamics. Over time, the interaction between cooling daytime and warming nighttime LST might necessitate adjustments in local climate adaptation strategies and policy approaches.

The readers must consider the limitations of the present study while interpreting the findings. The time of all the datasets in the present study is 1.30 and 13.30 intending to capture the maximum thermal contrast between daytime and nighttime LST. The mismatch of spatial resolution of the datasets can result in an underestimation or overestimation of LST trends, particularly in heterogeneous landscapes. Cloud cover in satellite-derived LST could hinder the understanding of regional climate variations, especially in regions where cloud cover is frequent. Reanalysis models' assumptions, such as the representation of land surface processes and boundary conditions, can introduce biases. If the assumptions do not accurately reflect local conditions, the model outputs may diverge from actual measurements, particularly in diverse climatic regions of India. Lastly, integrating datasets from different sources can introduce complexities, including discrepancies in data processing algorithms and methodologies. Variations in calibration and validation approaches can lead to inconsistencies between satellite and reanalysis outputs, complicating the interpretation of comparative trends. Future studies should consider integrating multiple satellite datasets to mitigate the discrepancies among datasets, ensuring more consistent and reliable LST estimates across regions. Higher-resolution satellite datasets, particularly those with finer spatial and temporal resolutions, can provide more detailed insights into regional variations in LST, especially in heterogeneous landscapes. Incorporating cloud cover correction algorithms could further improve the accuracy of satellite-derived LST estimates, particularly in regions with frequent cloud cover, where traditional satellite data may be obscured. Additionally, the integration of ground-based measurements through localized reanalysis models can help address biases caused by generalized assumptions in satellite data. These models, when combined with ground-based observations, allow for a more precise understanding of land surface processes and boundary conditions, which can refine predictions of LST and regional climate variations. By considering both higher-resolution data and ground-based measurements, future studies could provide a more accurate and context-specific understanding of LST, addressing current limitations related to data resolution, cloud cover, and regional variability.

5 Conclusions

The comparative analysis of daytime and nighttime LST and its trends in India (2003–2022) using satellite and reanalysis data has unveiled multifaceted insights into the dynamics of environmental changes within the region. The juxtaposition of these datasets has provided a nuanced understanding of LST variations across diverse landscapes, climatic zones, and temporal scales. The key findings of the present study are as follows-.

1. In both satellite and reanalysis datasets, the daytime mean LST exhibits the highest absolute values during

the pre-monsoon period, followed by the monsoon, post-monsoon, and winter seasons. In contrast, the nighttime mean LST reaches its highest levels during the monsoon season, followed by the pre-monsoon, post-monsoon, and winter seasons.

2. The comparison between satellite and reanalysis datasets (for daytime and nighttime mean LST) has revealed a strong correlation coefficient across all datasets. However, some of the other statistical indicators do not exhibit the expected values in certain comparisons.
3. One of the key observations from our analysis is the significant divergence in daytime mean LST trends between satellite and reanalysis data during various seasons. During winter, for instance, all datasets exhibit distinctive cooling trends in daytime mean LST across almost all climatic regions. However, notable discrepancies are observed in certain regions where reanalysis data show minute warming trends, highlighting potential differences in the representation of LST dynamics between the two data sources. Moreover, the nighttime mean LST also depicts a cooling trend in most parts of the study area across all datasets. Nevertheless, in certain regions of the P and NE, all datasets except ERA5-Land show a warming trend.
4. Daytime pre-monsoon trends reveal a similar pattern, with satellite data indicating cooling trends across all regions, while reanalysis data depict warming in some areas alongside cooling trends in others. This discrepancy underscores the importance of considering multiple datasets and their inherent uncertainties when analyzing temperature trends. Additionally, regarding the nighttime mean LST, there are noticeable variations between the datasets, although ERA5-Land and MERRA-2 are more consistent with each other.
5. During the monsoon season, both cooling and warming trends are evident in daytime mean LST across all datasets, with MODIS depicting cooling across all climatic regions and AIRS suggesting warming in certain areas. The existence of contrasting trends underscores the intricate interaction of multiple factors influencing LST dynamics during this season, such as precipitation patterns, cloud cover, and land-atmosphere interactions. Similarly, nighttime mean LST also exhibits both warming and cooling trends across all datasets.
6. The post-monsoon analysis highlights a declining trend in daytime mean LST across most regions, with notable exceptions where significant warming is observed in specific areas from reanalysis datasets. This discrepancy between satellite and reanalysis data underscores the need for careful consideration of data sources and their respective limitations when interpreting temperature trends. Regarding nighttime mean LST, all datasets primarily indicate a warming trend, although a few patches of cooling trend were there.

Overall, findings suggest that while satellite data provide consistent insights into LST trends at an annual scale, differences arise when comparing seasonal trends with reanalysis data. At an annual level, all datasets (except ERA5-Land) show comparable trends in daytime mean LST across their respective climate regions. However, variations are evident among the datasets in nighttime mean LST trends over specific regions. While both satellite-derived datasets (MODIS Aqua and AIRS Aqua) and reanalysis data (ERA5-Land and MERRA-2) have demonstrated commendable capabilities in tracking LST trends, disparities and discrepancies in certain regions and timeframes have been revealed. Satellite data exhibited higher spatial resolutions, capturing local-scale variations in LST, whereas reanalysis data portrayed broader-scale trends with varying degrees of accuracy. However, despite their differences, the convergence of trends in several key areas signifies a degree of agreement between the datasets, thereby reinforcing certain observed temperature trends. These findings underscore the importance of amalgamating multiple data sources for a comprehensive understanding of LST dynamics. The present study provides valuable insights into the diurnal variations in LST, which is crucial for understanding surface heat flux and energy balance in different environments. It contributes to the broader global discourse on climate change and underscores the significance of reliable, integrated data sources in shaping effective policies and strategies for sustainable land use and environmental conservation.

Acknowledgements The first author is thankful to the Banaras Hindu University, Varanasi, Uttar Pradesh (India), for providing the project grant (No. R/Dev/D/IoE/TDR-projects-II (Sanction)/2023-24/69592 to 69593) under the Institute of Eminence (IoE). Subhash Singh (Ref. No. 220510022095) is grateful to the University Grants Commission (UGC) of the Ministry of Education, Government of India (New Delhi) for providing financial support. The authors are thankful to the National Aeronautics and Space Administration (NASA), and the Copernicus Climate Change Service (C3S) for providing data in the public domain.

Author contributions All authors contributed to the study's conception, design, analysis, original draft writing - review & editing.

Funding The first author received the project grant from the Banaras Hindu University, Varanasi, Uttar Pradesh (India) (No. R/Dev/D/IoE/TDR-projects-II (Sanction)/2023-24/69592 to 69593) under the Institute of Eminence (IoE). Subhash Singh (Ref. No. 220510022095) received a fellowship from the University Grants Commission (UGC) of the Ministry of Education, Government of India (New Delhi).

Data availability The raw datasets of PWV used in the present study are available at ERA5-Land: https://cds.climate.copernicus.eu; MODIS Aqua: https://search.earthdata.nasa.gov; AIRS Aqua: https://daac.gsfc.nasa.gov; MERRA-2: https://daac.gsfc.nasa.gov.

Declarations

Competing interests The authors have no relevant financial or non-financial interests to disclose.

References

Bosilovich MG, Lucchesi R, Suarez M (2015) MERRA-2: File Specification. GMAO Office Note No. 9 (Version 1.0), 73 pp. Available via http://gmao.gsfc.nasa.gov/pubs/office_notes. Accessed 15 Jan 2024

Cai M, Ren C, Xu Y, Lau KKL, Wang R (2018) Investigating the relationship between local climate zone and land surface temperature using an improved WUDAPT methodology–A case study of Yangtze River Delta, China. Urban Clim 24:485–502. https://doi.org/10.1016/j.uclim.2017.05.010

Chaudhuri G, Mishra NB (2016) Spatio-temporal dynamics of land cover and land surface temperature in Ganges-Brahmaputra delta: A comparative analysis between India and Bangladesh. Appl Geogr 68:68–83. https://doi.org/10.1016/j.apgeog.2016.01.002

Choudhury A (2024) Drought trend and its association with land surface temperature (LST) over homogeneous drought regions of India (2001–2019). Discov Water 4:51. https://doi.org/10.1007/s43832-024-00115-8

Dimri AP (2019) Comparison of regional and seasonal changes and trends in daily surface temperature extremes over India and its subregions. Theor Appl Climatol 136:265–286. https://doi.org/10.1007/s00704-018-2486-5

Entekhabi D, Reichle RH, Koster RD, Crow WT (2010) Performance metrics for soil moisture retrievals and application requirements. J Hydrometeorol 11(3):832–840

Friedl M, Sulla-Menashe D (2022) MODIS/Terra + Aqua Land Cover Type Yearly L3 Global 500m SIN Grid V061. NASA EOSDIS Land Processes Distrib Act Archive Cent. https://doi.org/10.5067/MODIS/MCD12Q1.061. Accessed 01 January 2024

GCOS (2016) The Global Observing System For Climate: Implementation Needs GCOS-200 (GOOS-214)

Han X, Wang C (2021) Weakened feedback of the Indian Ocean on El Niño since the early 1990s. Clim Dyn 57(3):879–894. https://doi.org/10.1007/s00382-021-05745-5

IMD (2023) Terminologies and glossary. IMD. Available via https://img.indiaonline.in/weather/Weather-Glossary.pdf. Accessed 10 January 2024

Jiménez-Muñoz JC, Mattar C, Sobrino JA, Malhi Y (2016) Digital thermal monitoring of the Amazon forest: an intercomparison of satellite and reanalysis products. Int J Digit Earth 9(5):477–498. https://doi.org/10.1080/17538947.2015.1056559

Kendall MG (1975) Rank Correlation Methods. 4th Edition, Charles Griffin, London

Khandan R, Gholamnia M, Duan SB, Ghadimi M, Alavipanah SK (2018) Characterization of maximum land surface temperatures in 16 years from MODIS in Iran. Environ Earth Sci 77:1–11. https://doi.org/10.1007/s12665-018-7623-z

Latif Y, Yaoming M, Yaseen M, Muhammad S, Wazir MA (2020) Spatial analysis of temperature time series over the Upper Indus Basin (UIB) Pakistan. Theor Appl Climatol 139:741–758. https://doi.org/10.1007/s00704-019-02993-8

Lee YR, Yoo JM, Jeong MJ, Won YI, Hearty T, Shin DB (2013) Comparison between MODIS and AIRS/AMSU satellite-derived surface skin temperatures. Atmos Meas Tech 6(2):445–455. https://doi.org/10.5194/amt-6-445-2013

Li ZL, Tang BH, Wu H, Ren H, Yan G, Wan Z, Trigo IF, Sobrino JA (2013) Satellite-derived land surface temperature: Current status and perspectives. Remote Sens Environ 131:14–37. https://doi.org/10.1016/j.rse.2012.12.008

Li ZL, Wu H, Duan SB, Zhao W, Ren H, Liu X, Pei L, Tang R, Ye X, Zhu J, Sun Y, Si M, Liu M, Li J, Zhang X, Shang G, Tang B-H, Yan G, Zhou C (2023) Satellite remote sensing of global land surface temperature: Definition, methods, products, and applications. Rev Geophys. https://doi.org/10.1029/2022RG000777

Linacre E, Geerts B (1997) Climates and weather explained, vol 432. Routledge, London

Liu W, Chen S, Jiang H, Wang C, Li D (2017) Spatiotemporal Analysis of MODIS Land Surface Temperature With In Situ Meteorological Observation and ERA-Interim Reanalysis: The Option of Model Calibration. IEEE J Sel Top Appl Earth Obs Remote Sens 10(4):1357–1371. https://doi.org/10.1109/JSTARS.2016.2645859

Liu J, Hagan DFT, Liu Y (2020) Global land surface temperature change (2003–2017) and its relationship with climate drivers: AIRS, MODIS, and ERA5-land based analysis. Remote Sens 13(1):44. https://doi.org/10.3390/rs13010044

Liu Y, Yu Y, Wang H, Yu P (2023) Land surface temperature validation. In Field Measurements for Passive Environmental Remote Sensing. https://doi.org/10.1016/B978-0-12-823953-7.00016-2

Mal S, Rani S, Maharana P (2022) Estimation of spatiotemporal variability in land surface temperature over the Ganga River Basin using MODIS data. Geocarto Int 37(13):3817–3839. https://doi.org/10.1080/10106049.2020.1869331

Mal S, Agrawal K, Rani S, Maharana P, Raman VAV (2023) Evaluating spatial and elevation-wise daytime/nighttime LST trends across the Indus River Basin. J Mt Sci 20(11):3154–3172. https://doi.org/10.1007/s11629-023-8157-8

Mildrexler DJ, Zhao M, Running SW (2011) A global comparison between station air temperatures and MODIS land surface temperatures reveals the cooling role of forests. J Geophys Res: Biogeo. https://doi.org/10.1029/2010JG001486

Mishra V (2020) Long-term (1870–2018) drought reconstruction in context of surface water security in India. J Hydrol. https://doi.org/10.1016/j.jhydrol.2019.124228

Mukherjee F, Singh D (2020) Assessing land use–land cover change and its impact on land surface temperature using LANDSAT data: A comparison of two urban areas in India. Earth Syst Environ 4, 385–407 (2020). https://doi.org/10.1007/s41748-020-00155-9

Muñoz-Sabater J, Dutra E, Agustí-Panareda A, Albergel C, Arduini G, Balsamo G, Boussetta S, Choulga M, Harrigan S, Hersbach H, Martens B, Miralles DG, Piles M, Rodríguez-Fernández NJ, Zsoter E, Buontempo C, Thépaut JN (2021) ERA5-Land: a state-of-the-art global reanalysis dataset for land applications. Earth Syst Sci Data 13:4349–4383. https://doi.org/10.5194/essd-13-4349-2021

Naikoo MW, Islam ARMT, Mallick J, Rahman A (2022) Land use/land cover change and its impact on surface urban heat island and urban thermal comfort in a metropolitan city. Urban Clim 41:101052. https://doi.org/10.1016/j.uclim.2021.101052

National Remote Sensing Centre (2024) LAND USE LAND COVER 2005-06 and 2022-23. Bhuvan. https://bhuvan-app1.nrsc.gov.in/thematic/thematic/index.php

Neeti N, Eastman JR (2011) A contextual mann-kendall approach for the assessment of trend significance in image time series. Trans GIS 15(5):599–611. https://doi.org/10.1111/j.1467-9671.2011.01280.x

Null J (2024) El Niño and La Niña Years and Intensities Based on Oceanic Niño Index (ONI). https://ggweather.com/enso/oni.htm

Pal I, Al-Tabbaa A (2010) Long-term changes and variability of monthly extreme temperatures in India. Theor Appl Climatol 100:45–56. https://doi.org/10.1007/s00704-009-0167-0

Prakash S, Norouzi H (2020) Land surface temperature variability across India: a remote sensing satellite perspective. Theor Appl

Climatol 139:773–784. https://doi.org/10.1007/s00704-019-03010-8
Rani S, Mal S (2022) Trends in land surface temperature and its drivers over the High Mountain Asia. Egypt J Remote Sens Space Sci 25(3):717–729. https://doi.org/10.1016/j.ejrs.2022.04.005
Rani S, Singh J, Singh S, Tiwari P, Mal S (2023) Decadal trends in precipitable water vapor over the Indus River Basin using ERA5 reanalysis data. J Mt Sci 20(10):2928–2945. https://doi.org/10.1007/s11629-023-8112-8
Rani S, Maharana P, Mal S (2024) Assessing the Monthly Trends in Precipitable Water Vapor over the Indian Subcontinent. Ann Am Assoc 114(4):671–696. https://doi.org/10.1080/24694452.2023.2294899
Rao P, Gupta K, Roy A, Balan R (2021) Spatio-temporal analysis of land surface temperature for identification of heat wave risk and vulnerability hotspots in Indo-Gangetic Plains of India. Theor Appl Climatol 146:567–582. https://doi.org/10.1007/s00704-021-03756-0
Retamales-Muñoz G, Durán-Alarcón C, Mattar C (2019) Recent land surface temperature patterns in Antarctica using satellite and reanalysis data. J South Am Earth Sci 95:102304. https://doi.org/10.1016/j.jsames.2019.102304
Sen PK (1968) Estimates of the regression coefficient based on Kendall's Tau. J Am Stat Assoc 63:1379–1389. https://doi.org/10.1080/01621459.1968.10480934
Shahfahad, Rihan M, Naikoo MW, Ali MA, Usmani TM, Rahman A (2021) Urban heat island dynamics in response to land-use/land-cover change in the coastal city of Mumbai. J Indian Soc Remote Sens 49(9):2227–2247. https://doi.org/10.1007/s12524-021-01394-7
Sharifnezhadazizi Z, Norouzi H, Prakash S, Beale C, Khanbilvardi R (2019) A global analysis of land surface temperature diurnal cycle using MODIS observations. J Appl Meteorol Climatol 58(6):1279–1291. https://doi.org/10.1175/JAMC-D-18-0256.1
Siddiqui A, Kushwaha G, Nikam B, Srivastav SK, Shelar A, Kumar P (2021) Analysing the day/night seasonal and annual changes and trends in land surface temperature and surface urban heat island intensity (SUHII) for Indian cities. Sustain Cities Soc 75:103374. https://doi.org/10.1016/j.scs.2021.103374
Singh S, Kumar P, Parijat R, Gonengcil B, Rai A (2024) Establishing the relationship between land use land cover, normalized difference vegetation index and land surface temperature: A case of Lower Son River Basin, India. Geogr Sustain 5(2):265–275. https://doi.org/10.1016/j.geosus.2023.11.006
Sultana S, Satyanarayana ANV (2018) Urban heat island intensity during winter over metropolitan cities of India using remote-sensing techniques: Impact of urbanization. Int J Remote Sens 39(20):6692–6730. https://doi.org/10.1080/01431161.2018.1466072
Susskind J, Schmidt GA, Lee JN, Iredell L (2019) Recent global warming as confirmed by AIRS. Environ Res Lett 14(4):044030. https://doi.org/10.1088/1748–9326/aafd4e
Theil H (1950) A rank-invariant method of linear and polynomial regression analysis. Indag Math 12(85):173
Thrastarson HD, Fetzer E, Lambrigtsen B, Manning E, Yue Q, Tian B, Milstein A (2020) AIRS/AMSU/HSB version 7 changes from version 6. Jet Propulsion Laboratory. Retrieved from https://docserver.gesdisc.eosdis.nasa.gov/public/project/AIRS/V7_Changes_from_V6. pdf. Accessed 08 Dec 2024
Thrastarson HT, Fetzer EF, Ray S, Hearty T, Smith N (2021) Overview of the AIRS mission: instruments, processing algorithms, products, and documentation. Jet Propulsion Laboratory California Institute of Technology, Pasadena, CA, https://docserver.gesdisc.eosdis.nasa.gov/public/project/AIRS/Overview_of_the_AIRS_Mission. pdf, Accessed 08 Dec 2024
Tian B, Manning E, Roman J, Thrastarson H, Fetzer E, Monarrez R (2020) AIRS version 7 level 3 product user guide. Jet Propulsion Laboratory, California Institute of Technology. Available via https://airs.jpl.nasa.gov/data/products/v7-L2-L3/. Accessed 03 Feb 2024
Trigo IF, Monteiro IT, Olesen F, Kabsch E (2008) An assessment of remotely sensed land surface temperature. J Geophys Res: Atmos. https://doi.org/10.1029/2008JD010035
Vinnarasi R, Dhanya CT, Chakravorty A, AghaKouchak A (2017) Unravelling diurnal asymmetry of surface temperature in different climate zones. Sci Rep 7(1):7350. https://doi.org/10.1038/s41598-017-07627-5
Wan Z (1999) MODIS land-surface temperature algorithm theoretical basis document (LST ATBD). Institute for Computational Earth System Science. Santa Barbara 75:18
Wan Z (2019) Collection-6 MODIS land surface temperature products users' guide. ICESS, University of California, Santa Barbara, p 400
Wang YR, Hessen DO, Samset BH, Stordal F (2022) Evaluating global and regional land warming trends in the past decades with both MODIS and ERA5-Land land surface temperature data. Remote Sens Environ 280:113181. https://doi.org/10.1016/j.rse.2022.113181
Wen A, Wu T, Wu X, Zhu X, Li R, Ni J, Hu G, Qiao Y, Zou D, Chen J, Wang D, Lou P (2022) Evaluation of MERRA-2 land surface temperature dataset and its application in permafrost mapping over China. Atmos Res 279:106373. https://doi.org/10.1016/j.atmosres.2022.106373
Yang S, Li R, Wu T, Hu G, Xia Y, Du Y, Zhu X, Ni J, Ma J, Zhang Y, Shi J, Qiao Y (2020) Evaluation of reanalysis soil temperature and soil moisture products in permafrost regions on the Qinghai-Tibetan Plateau. Geoderma 377:114583. https://doi.org/10.1016/j.geoderma.2020.114583
Zhang X, Zhou J, Liang S, Wang D (2021) A practical reanalysis data and thermal infrared remote sensing data merging (RTM) method for reconstruction of a 1-km all-weather land surface temperature. Remote Sens Environ 260:112437. https://doi.org/10.1016/j.rse.2021.112437
Zhao W, He J, Wu Y, Xiong D, Wen F, Li A (2019) An analysis of land surface temperature trends in the central Himalayan region based on MODIS products. Remote Sens 11(8):900. https://doi.org/10.3390/rs11080900
Zhou C, Wang K (2016) Land surface temperature over global deserts: Means, variability, and trends. J Geophys Res: Atmos 121(24):14–344. https://doi.org/10.1002/2016JD025410